12-1997

PAN, PPN and MPAN Measurements and the Systematic Relationship between MPAN and MACR at a Semi-Rural Site in Tennessee

George Nouaime
Western Michigan University

PAN, PPN AND MPAN MEASUREMENTS AND THE SYSTEMATIC RELATIONSHIP BETWEEN MPAN AND MACR AT A SEMI-RURAL SITE IN TENNESSEE

by

George Nouaime

A Thesis
Submitted to the
Faculty of The Graduate College
in partial fulfillment of the
requirements for the
Degree of Master of Arts
Department of Chemistry

Western Michigan University
Kalamazoo, Michigan
December 1997

To
the love of Hiam
and
the memory of Assaf

ACKNOWLEDGMENTS

I would like to express my deepest appreciation and gratitude to my advisor, Dr. Steven Bertman, for his patience and guidance and for the opportunity to work with him. The exposure I had through Dr. Bertman's research group to science and to people of different backgrounds was an essential part in preparing me for a world beyond WMU's campus. I am also very grateful to the members of my committee, Dr. Susan Burns and Dr. Michael Dziewatkoski, for their time and helpful suggestions which were essential to my work.

I would also would like to thank Dr. Paul Shepson, Dr. Ken Olszyna, Dr. Rod Zika, the National Oceanic and Atmospheric Administration (NOAA) and the Southern Oxidants Study (SOS) community for their help and/or for allowing the use of their data in this thesis. Special thanks go to Deanna Elyea, Heidi Huang and Craig Seaver for helping out in the PANs measurement during the 1995 SOS Intensive in Nashville. The PANs measurement was supported by the US EPA through a subcontract with Georgia Institute of Technology.

Finally, I would like to acknowledge my family, relatives and friends for their constant support and without whom my success would not have been possible. In particular two people come to mind: Aunt Helen Rogers, an exemplary woman, who accepted me in her home as her own son when I returned to the United States for college, and my patient wife Liz who was always there for me with encouragement and advice during the course of my degree.

George Nouaime

PAN, PPN AND MPAN MEASUREMENTS AND THE SYSTEMATIC RELATIONSHIP BETWEEN MPAN AND MACR AT A SEMI-RURAL SITE IN TENNESSEE

George Nouaime, M.A.

Western Michigan University, 1997

Simultaneous measurements of peroxymethacryloyl nitrate (MPAN) and its primary and secondary precursors, methacarolein (MACR) and isoprene, were carried out for the first time in July 1995 at a semi-rural site southeast of Nashville. In addition to these compounds, peroxyacetyl nitrate (PAN), peroxypropionyl nitrate (PPN), other volatile organic compounds (VOCs) and supporting measurements were also collected in collaboration with other research groups. The mean concentrations of PAN, PPN, MPAN and MACR were found to be 485 pptv, 50 pptv, 30 pptv and 0.290 ppbv respectively. MPAN levels, which closely tracked those of MACR during the day, peaked and dropped earlier than PAN, PPN and ozone levels. The morning peaks in MACR and MPAN appear to be due to a combination of active photochemical synthesis and downward mixing of both compounds as the nocturnal boundary layer breaks up. There are daytime periods when MPAN and MACR do not correlate well and this appears to be associated with a combination of high NO_2, high NO_2/NO, and limited OH production which may simultaneously decrease MACR production and increase MPAN lifetime. Unlike PAN, MPAN did not correlate well with O_3, constituted less than 1% of NOy and appeared to have a shorter ambient lifetime. This indicates that MPAN may not be a significant reservoir and transporter of NO_X at Youth Inc.. As a result, ozone production through MPAN decomposition may be limited locally which makes MPAN a useful indicator of local biogenic photochemistry.

TABLE OF CONTENTS

Table of Contents—continued

LIST OF TABLES

LIST OF FIGURES

List of Figures—continued

CHAPTER I

INTRODUCTION

Peroxyacyl Nitrates: Background and Characteristics

Peroxyacyl nitrates (PANs) are atmospheric products of the photochemical oxidation of volatile organic compounds (VOCs) in the presence of NO_x ($NO + NO_2$). Sources of NO_x include fossil fuel combustion, soil emissions and lightning. PANs have a general formula of $RC(O)OONO_2$. Peroxyacetyl nitrate, PAN (Figure 1), is the simplest PAN compound and was first discovered in the atmosphere by Stephens et al. in the 1950's through long-path infrared spectroscopy (Altshuller, 1993; Scott et al., 1957; Stephens et al., 1956). Other significant PAN compounds that have been detected in the atmosphere include peroxypropionyl nitrate (PPN) peroxymethacryloyl nitrate (MPAN) and peroxybenzoyl nitrate (PBzN) (Figure 1).

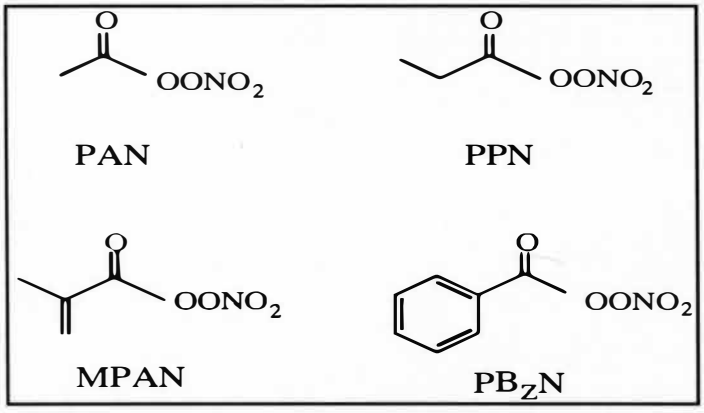

Figure 1. Chemical Structures of PAN, PPN, MPAN and PBzN.

While many measurements of PAN have been made since Stephens first reported it, peroxypropionyl nitrate (PPN) measurements are less common. A number of papers provide good summaries of PAN and PPN measurements (Altshuler, 1983; Temple and Taylor, 1983; Grosjean, 1984; Roberts, 1990). Even fewer measurements of peroxybenzoyl nitrate (PBzN) are available due to low concentrations in the air and analytical difficulties (Appel, 1973; Meijer and Nieboer, 1976; Fung and Grosjean, 1985).

Peroxyacyl nitrates are of importance in atmospheric chemistry and need to be studied closely. PANs constitute a significant percentage of the total atmospheric nitrogen budget (NOy). They have a relatively long lifetime in the troposphere and can, as a result, be transported over long distances before thermally decomposing into a peroxy radical (RC(O)OO•) and NO_2. Thus PANs can act as reservoirs for NOx (NO_2 and NO) and radicals. In turn, NO_2 can photolyze to produce NO and ozone through the following reactions:

$$NO_2 + h\upsilon \longrightarrow O(^3P) + NO \qquad (1)$$

$$O(^3P) + O_2 \longrightarrow O_3 \qquad (2)$$

Therefore through transport, PANs have the potential of creating ozone in areas other than where they were produced.

In addition to their role in NOx transport and ozone production, peroxyacyl nitrates are a health hazard to plants and animals, causing crop damage, eye irritation, mutagenicity and possibly skin cancer (Stephens, 1969; Temple and Taylor, 1983; Kliendienst et al, 1990; Altshuller, 1993; Heddle et al, 1993).

PANs Chemistry

The hydrocarbon precursors of PANs, which can be emitted by either anthropogenic or biogenic sources, are eventually oxidized into other formsthrough a series of radical reactions starting with hydrogen abstraction by hydroxyl radicals in the presence of oxygen (equation 3).

$$RH + \bullet OH + O_2 \longrightarrow ROO\bullet + H_2O \qquad (3)$$

Hydroxyl radicals are the main atmospheric species that drive the chemistry of the troposphere in the daytime and the leading species responsible for the loss of hydrocarbons (Finlayson-Pitts and Pitts, p. 629, 1986). The main source of OH radicals is the photolysis of ozone in the presence of water, which produces two hydroxyl radicals. The photolysis of HCHO, H_2O_2 and HONO also result in OH formation. In the presence of sufficient NOx, the alkylperoxy radicals (ROO•) from reaction (3) react with NO to produce either alkoxy radicals (RO•) or alkyl nitrates ($RONO_2$) (equations 4 and 5).

$$ROO\bullet + NO \longrightarrow RO\bullet + NO_2 \qquad (4)$$

$$ROO\bullet + NO \longrightarrow RONO_2 \qquad (5)$$

Oxygen reacts quickly with the RO• radical yielding a carbonyl compound and a hydroperoxy radical ($HO_2\bullet$). In the case where aldehydes are formed (equation 6), an OH radical can abstract the carbonyl hydrogen of aldehydes in the presence of oxygen to generate an acyl peroxy radical (RC(O)OO•) (equation 7).

$$RO\bullet + O_2 \longrightarrow RC(O)H + HOO\bullet \qquad (6)$$

$$RC(O)H + \bullet OH + O_2 \longrightarrow RC(O)OO\bullet + H_2O \qquad (7)$$

Nitrogen dioxide can react with RC(O)OO• to generate peroxyacyl nitrates, which is in equilibrium with the thermal dissociation of PANs (equation 8).

$$RC(O)OO\bullet + NO_2 \rightleftharpoons RC(O)OONO_2 \qquad (8)$$

The process leading to PAN formation (equations 3 - 8) indirectly generates ozone. Equations 3, 6, and 7 produce ROO•, HOO•, and RC(O)OO• respectively which react with NO to produce RO•, HO•, RC(O)O• and three NO_2 molecules that translate through photolysis into three ozone molecules. RO•, HO• can then re-enter the cycle through equations 3, 7 and 8 where more ozone molecules can be formed. RC(O)O• can react with NO_2 to produce RC(O)OO• which can form PAN in the presence of another NO_2 molecule.

PANs Precursors

Knowing the distribution and the chemistry of the PAN precursors, anthropogenic and biogenic, can help determine their role in photochemical smog formation. One way to do this is through simultaneous ambient measurements of VOCs and their PAN products. Through VOC measurements, Biesenthal et al. (1997a) were able to detect an anthropogenic source of MPAN's precursor methacrolein, MACR, which is chiefly a biogenic oxidation product. Simultaneous measurements of PAN, PPN and MPAN allow the determination of the extent of biogenic and anthropogenic contribution to PAN and ozone production since the three PANs have different origins (Williams et al., 1997b; Roberts et al., 1997).

Most two carbon alkyl radicals produced from the photooxidation of larger biogenic and anthropogenic VOCs, can lead to PAN formation. For example, PAN

can be formed from the photooxidation of the biogenic compound isoprene (Tuazon and Atkinson, 1990b). Ethane, 2-butene, acetone, biacetyl, methyl glyoxal and acetaldehyde among others also oxidize to form PAN (Finlayson-Pitts and Pitts, 1986). Therefore anthropogenic and biogenic VOCs may both be significant in producing PAN depending on their relative levels at any given time of the day.

PPN is present in the atmosphere with concentrations of about an order of magnitude less than PAN's (Finlayson-Pitts and Pitts, p. 553, 1986). This is primarily because the VOC sources of PAN are more abundant than the VOC precursors of PPN (Roberts, 1990). PPN sources include propane, methyl ethyl ketone, propanal and other larger hydrocarbons which are mainly anthropogenic. Biogenic sources of PPN, such as cis-3-Hexen-1-ol, have been discussed (Grosjean et al., 1993b; Aschmann et al., 1997) but have not been shown to be significant. The ratio of PPN to PAN is higher in urban areas than in rural and remote areas which indicates that the dominant source of PPN is anthropogenic (Altshuller, 1993). PPN therefore may be used as a marker of anthropogenic photochemical activity.

In contrast to PPN, MPAN production is mostly due to biogenic photochemistry. MPAN has been characterized (Bertman and Roberts, 1991) and measured to a limited extent in the southeastern United States (Williams et al., 1993; Roberts et al., 1997). The only source of MPAN in the atmosphere is methacrolein, MACR (Figure 2), which is a primary oxidation product of isoprene (Figure 2) (Aschmann and Atkinson, 1994; Bertman and Roberts, 1991). Isoprene is an unsaturated hydrocarbon released mainly by deciduous trees and its emissions, which are temperature and light dependent, peak in mid-summer in the northern hemisphere. Automobile exhaust has been found to contain MACR (Biesenthal, 1997a), but isoprene is considered to be the dominant source of MACR to the atmosphere in the

summer (Starn et al., 1997b, Montzka, 1993), which makes MPAN an indicator of biogenic photochemistry. Isoprene reacts with hydroxyl radicals and ozone to produce both methacrolein (MACR) and methyl vinyl ketone (MVK) (Figure 2) (Tuazon and Atkinson, 1990b). Daytime isoprene chemistry is dominated by OH radicals, while ozone chemistry becomes more significant at night. MACR reacts with OH in the presence of NO_2 to produce MPAN (Tuazon and Atkinson, 1990a).

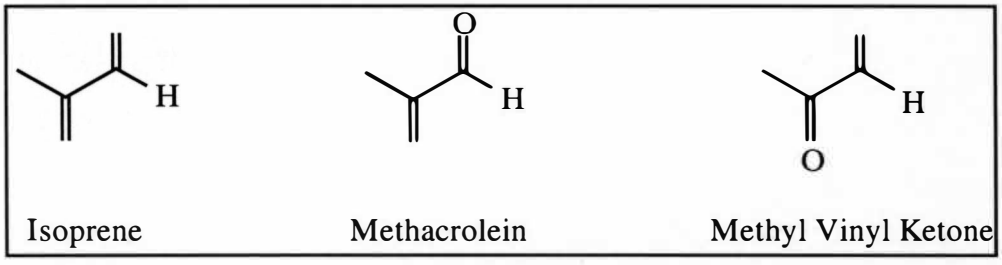

Figure 2. Chemical Structures of Isoprene, MACR and MVK.

The southeastern United States is an ideal location where isoprene and its oxidation products can be studied, because it is an area rich in vegetation where climatic and chemical conditions lead to significant tropospheric smog formation and ozone levels (Chameides and Cowling, 1995). Such conditions include a combination of high summer temperatures, high solar radiation, high humidity, air stagnation, and an abundance of NO_x and hydrocarbons sources.

Research Objectives

The elevated levels of ozone in the southeastern United States are the target of the Southern Oxidants Study (SOS), a long term study dedicated to understanding the reasons behind the accumulation of high ozone concentrations in that region. SOS consists of a group of researchers from the academic, private, federal and state sectors working together since 1988 on a long term basis at a number of chosen southern

cities. Between 1990 and 1995, a number of pilot studies were conducted in Durham, Raleigh, Atlanta, Tampa, Birmingham and Nashville, along with intensive studies in Atlanta in 1992 and in Nashville in 1994 and 1995. Each study included multiple sites where different aspects of the ozone problem were looked at. Besides ozone, measurements were made of other compounds and meteorological parameters related to ozone formation or transport, such as hydrocarbons, NOx, NOy, PANs, CO, temperature, solar flux and wind speed and direction among others.

During the 1995 Nashville/Middle Tennessee Ozone Study, PANs measurements were made by Dr. Steven Bertman's group (Western Michigan University), at a semi-rural forested site in the Nashville area. Local isoprene emissions from trees combined with the regular impact of urban air masses at this site make this site an ideal location to monitor both anthropogenic and biogenic photochemistry. Data collection of other supporting measurements including VOCs, ozone and NOx were conducted by other participating groups. This collaborative effort resulted in the first simultaneous measurements of isoprene, MACR and MPAN as well as propanal and PPN.

Analysis of the levels of MPAN and its precursors MACR and isoprene, along with other data collected at Youth Inc., should help provide information about the impact of isoprene photochemistry on oxidant production. While one of the main objectives at this site is to assess isoprene's contribution to ozone formation, the goals of this thesis are to characterize the systematic behavior of PAN, PPN and MPAN, with special attention on the relationship between MPAN and MACR. An improved synthetic and purification procedure for MPAN standards will also be described.

CHAPTER II

EXPERIMENTAL SECTION

Measurement Site

The PAN measurements were made between June 29 and July 26, 1995 at the Youth Inc. Ranch in Lavergne, TN. This site was located approximately 30 km southeast of downtown Nashville on a peninsula of the Percy Priest Reservoir at an elevation of about 150 m above sea level. The instrumentation was placed in a trailer located in an open field which was surrounded by dense vegetation in the form of deciduous trees and ground cover in a semi-rural area where the effect of both biogenic and anthropogenic photochemistry could be detected. To the East and North of the site, across the reservoir, stood the Cedars of Lebanon State Forest. To the South were the small communities of Lavergne and Smyrna (about 9.7 km away). Located downwind of Nashville, the site was routinely impacted by urban NOx as well as local natural hydrocarbons.

Table 1 lists the main compounds that were measured at the Youth Inc. site and which are pertinent to this thesis. Also listed are the measurement methods and the research groups that took the measurements. The instruments automatically sampled air from a high volume glass column (I.D. = 2 in)which drew air from a height of 22 m at a flow of 2000 lpm (liters per minute). PANs were sampled at the rate of 4/hour. The isoprene, MVK and MACR measurements, described in Starn et al. (1997b), were performed at half hour intervals. O_3, NO, NO_2 and NOy were measured once every five minutes using commercially available instruments (TECO). In addition to these

compounds, the meteorological data used in this thesis were collected by the National Oceanic and Atmospheric Administration (NOAA) at a sampling frequency of 2/minute.

Table 1

List of Some of the Compounds Measured at Youth Inc.

Compound	Method	Primary Investigator	Affiliation
PAN	GC/ECD	S.B. Bertman	Westem Michigan University
PPN	GC/ECD	S.B. Bertman	Westem Michigan University
MPAN	GC/ECD	S.B. Bertman	Westem Michigan University
Isoprene	GC/MS	P.B. Shepson	Purdue University
MACR	GC/MS	P.B. Shepson	Purdue University
MVK	GC/MS	P.B. Shepson	Purdue University
O_3	UV Absorption	K. Olszyna	Tennessee Valley Authority
NO_2	Photolytic Cell followed by Chemiluminescence	K. Olszyna	Tennessee Valley Authority
NO	O_3 Chemiluminescence	K. Olszyna	Tennessee Valley Authority

PANs Instrumentation

PAN measurements were made using a custom built gas chromatograph (GC) designed to automatically sample whole air samples. GC automation and data acquisition regarding flow rates and the times samples was accomplished with a 16 bit A/D board using LabView software (National Instruments). Chromatograms were

recorded on an HP 3396 integrator, and saved on computer and analyzed using Chrom Perfect software (Justice Innovations).

The custom built GC was equipped with a Shimadzu GC Mini-2 electron capture detector (ECD) with a ^{63}Ni source that was maintained at 55 °C. The column, a DB-210 Megabore (J & W Scientific, l = 15 m, I.D. = 0.53 mm, thickness = 1 μm), was wrapped around an aluminum block which was cooled using thermoelectrics and set at 20 °C to minimize the thermal decomposition of PAN compounds. Helium and nitrogen were used as carrier and make-up gases respectively with flow rates set at 10 cc/min and 8 cc/min respectively. The gas chromatograph automatically sampled 1 cc of ambient air over a period of 20 seconds in 15 minute intervals using a Hamilton Teflon six-port rotary valve with an 1/8 inch PFA Teflon sample loop.

Figure 3 shows the flow diagram from which the GC/ECD sampled air. A Teflon diaphragm pump (KNF Neuberger) was used to continuously pump a smaller flow of air from the base of the glass inlet through 1/4 inch PFA Teflon tubing at a flow of approximately 1 SLPM (standard liter per minute). The GC sampled air at a rate of 50 SCCM (standard cc per minute) from this 1/4 inch line . The detection limit was 2 to 5 pptv and the uncertainty of the measurements with respect to PAN, PPN and MPAN were 20%, 25%, 30% respectively.

PANs GC Calibration

PAN, PPN, and MPAN calibrations were performed prior to and during the campaign using standards which were synthesized in the laboratory in either dodecane or tridecane (Nielsen et al., 1982; Gaffney et al., 1984) and stored in a freezer until needed. Using liquid PAN standards for instrument calibration is convenient and is "the method of choice" (Gaffney et al., 1989). For example, frozen liquid standards

are synthesized in the lab and then transported frozen to the field with ease. Once thawed and kept at 0 ^{o}C, the standard is ready for use and lasts for weeks provided that its temperature remains at 0 ^{o}C.

By placing the standards in diffusion cells at 0 °C, a continuous source of any of the three PANs was supplied to the GC for calibrations. Gaseous PANs diffuse up the diffusion cell capillary where they eventually mix into a continuous flow of zero air before being introduced to the GC. To perform a calibration, ambient PANs are first decomposed by passing ambient air through a heated coil at 150 °C -175 °C (Figure 3), approximately 65 cm in length, followed by the introduction of the gaseous PAN standards downstream from the coil so that only the PAN standards can be detected by the gas chromatograph. By altering the flow of air through the 1/4 inch tubing, different PAN mixing ratios are detected by the GC due to different dilution ratios, and therefore a multi-point calibration curve was obtained.

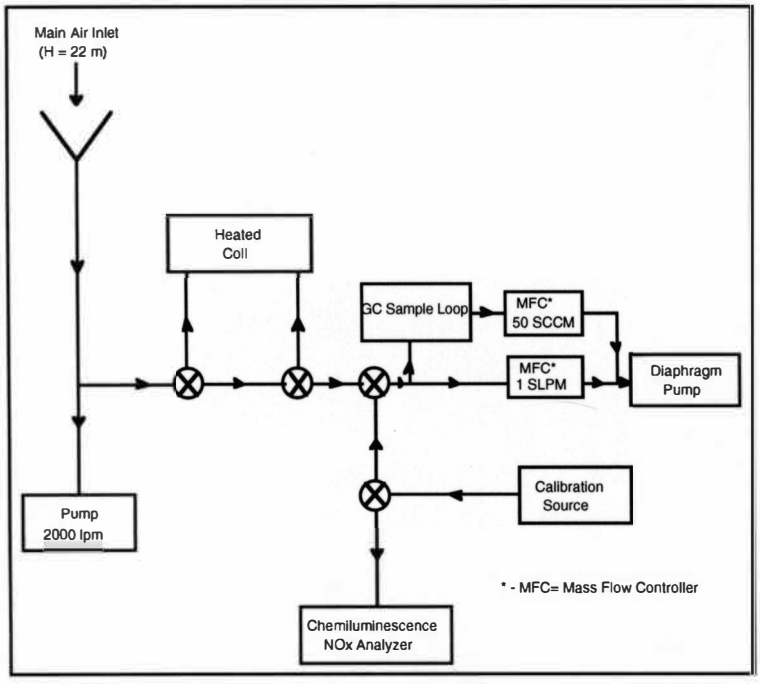

Figure 3. PAN GC/ECD Flow System Set-up.

The concentrations of the different PAN standards were measured by a Model 42S NO-NO_2-NOx chemiluminescence analyzer made by Thermo Environmental Instruments. Peroxyacyl nitrates from the calibration sources were directed to this analyzer where they undergo a conversion into NO at approximately 325 °C in the presence of a molybdenum catalyst. Nitric oxide molecules then react with ozone to produce excited state NO_2 molecules which upon relaxation emit light (equation 9).

$$NO + O_3 \longrightarrow NO_2^* \longrightarrow NO_2 + O_2 + h\nu \qquad (9)$$

The intensity of the light is proportional to the concentration of nitric oxide that is converted to nitrogen dioxide. Calibration of the NOx analyzer is done using a pure source of nitric oxide of known concentration (NIST Traceable Std Mixture, Scott Specialty).

To minimize uncertainties caused by PAN standard impurity: (a) HNO_3 is extracted from liquid PAN standards into water during synthesis; (b) nylon thread is used to scrub any unextracted HNO_3 by placing it into the Teflon tubing that transports PAN vapors from the diffusion cell to the analyzer; and (c) Fresh liquid PAN standards are used since they are less likely to breakdown into alkyl nitrates and NO_2 in large amounts. Uncertainties in flow rates, conversion efficiency of the molybdenum converter, the concentration of NO calibration standard could all contribute to the uncertainty of the instrument.

PAN, PPN and MPAN Syntheses

The syntheses of the peroxyacyl nitrates standards that were used in Nashville are based on the synthetic procedure that is reported by Nielsen et al. (1982) and

Gaffney et al. (1984). A percarboxylic acid in a heavy hydrocarbon such as dodecane or tridecane is nitrated in situ at 0 °C to produce a PAN compound (equation 10).

$$\text{R-C(O)OOH} + \text{H}_2\text{SO}_4/\text{HNO}_3 + \text{solvent} \longrightarrow \text{R-C(O)OONO}_2 \quad (10)$$

The peroxyacyl nitrate solutions are then stored in the freezer until needed.

Since peracetic acid is commercially available, PAN can be synthesized in one step; however, the synthesis of PPN and MPAN requires an additional step. Reacting propionic and methacrylic anhydrides with hydrogen peroxide and H_2SO_4 as catalyst produces perpropionic and permethacrylic acids (11), which then go through reaction (10) to produce PPN and MPAN respectively.

$$\text{R-C(O)OC(O)-R} + \text{H}_2\text{O}_2 + \text{H}^+ \longrightarrow \text{R-C(O)OOH} + \text{R-C(O)OH} \quad (11)$$

The syntheses of PAN and PPN are straightforward and provide consistent concentration levels for calibrations, but the MPAN synthesis can be problematic because MPAN yields are inconsistent and low. In addition, the synthesis is complicated by the formation of polymerization products and PAN as impurity. The polymerization products, which are non-existent in the PAN and PPN procedures, are due to the reactivity of the double bond of the R group. The mechanism in which PAN is formed has not yet been determined, but the presence of PAN dictates that the impure MPAN solutions be purified before they can be used for instrument calibration. If not removed, PAN can interfere with MPAN calibrations when the concentration of the standard is measured by chemiluminescence, as discussed above. An improved synthetic and purification procedure that provides consistent MPAN concentrations based on Bertman and Roberts (1991) will be described next.

MPAN Synthesis

5 ml of methacrylic anhydride (94%, Aldrich) were added to a 100 ml round bottom flask in an ice water bath. After 10 minutes, 50 µl of cold concentrated H_2SO_4 was added along the walls of the round bottom flask in small aliquots using a 10 µl syringe. The color of the solution turned to a faint orange-pink following the addition of sulfuric acid. The contents were stirred for an additional 10 minutes after which 0.6 ml of cold H_2O_2 (50 % wt., Aldrich) were slowly added dropwise along the sides of the round bottom flask. It is essential that the H_2O_2 be added as slowly as possible in order to avoid overheating the reaction mixture. The contents were stirred for 8 to 9 hours, during which the ice gradually warmed to room temperature. Meanwhile, 0.8 ml of each of concentrated sulfuric acid and fuming nitric acid (>90% wt.) were kept in the freezer in 1/2 dram vials for the nitration step. After 9 hours, the ice was replaced and the reactive mixture was stirred for 10 minutes, followed by the addition of 10 ml of cold tridecane (99+%, Aldrich). The mixture was stirred again for an additional 10 minutes. The 0.8 ml of cold concentrated sulfuric acid were added dropwise along the walls of the flask roughly at a rate of 1 to 2 drops every 10 to 15 seconds. Two minutes after H_2SO_4 addition, the 0.8 ml of cold fuming nitric acid were added dropwise also at a rate of approximately 1 to 2 drops every 10 to 15 seconds. The mixture was allowed to stir for an extra 8 to 10 minutes. The contents were then poured into a cold 125 ml separatory funnel containing 50 ml of ice cold water. The organic layer had a light yellow tint and the bottom of the aqueous layer contained yellow globules, which are probably polymeric by-products. The aqueous layer was immediately drained and the organic layer was washed twice with 25 ml of ice cold water, the second time with vigorous shaking. The organic layer was then transferred to a cold 100 ml beaker kept in ice and dried with as little anhydrous $MgSO_4$ as

possible. The organic layer was filtered through a long stem funnel containing a glass wool plug into vials cooled in ice and then frozen.

MPAN Purification

A slurry of silica gel, mesh 200-400, 60 Å (Aldrich) was prepared in methanol in a 100 ml beaker. The slurry was then poured into a 28 cm glass column with an internal diameter of 0.9 cm containing a glass wool plug at the base. The resulting gel column, 14.7 cm in length, was successively washed with 20 ml of acetone, 20 ml ethyl acetate, 25 ml of hexane and 35 ml of dodecane, using nitrogen (~40 PSI) to force the solvents through the gel. The gel became translucent after it was washed with dodecane. A small layer of dodecane was kept above the gel (1-2 cm high). The glass column was subsequently plugged to prevent dodecane evaporation and placed in the refrigerator to cool. Cooling the column prior to purification was done to minimize the thermal decomposition of MPAN. Once cooled, the column was removed from the refrigerator and a small amount of dodecane was drained to leave a minute layer above the gel. At that point, 2 ml of cold crude MPAN solution was added to the column and 2.5 ml fractions were collected immediately in cooled vials using cold dodecane as eluent.

The GC system described earlier was used to check the contents of each fraction. Opposite to the behavior on the GC column, MPAN eluted before PAN from this particular silica gel column. It is possible that MPAN is more soluble in dodecane than PAN is or that PAN is just retained longer on the gel. Reproducing the procedure so that pure MPAN always eluted in the same fractions and with the similar concentrations was not possible. This could be due to differences in the packing of the gel in the column, differences in the concentrations of the crude samples, variations in

the nitrogen pressure. Figure 4 shows an impure MPAN standard chromatogram containing both MPAN and PAN. Figure 5 shows the chromatograms of pure MPAN fractions from one purification procedure. Pure MPAN was found in fractions 7-11 in this particular purification. Neither PAN or MPAN were observed in fractions 1-6. PAN was not observed since it elutes after MPAN and only 11 fractions were collected.

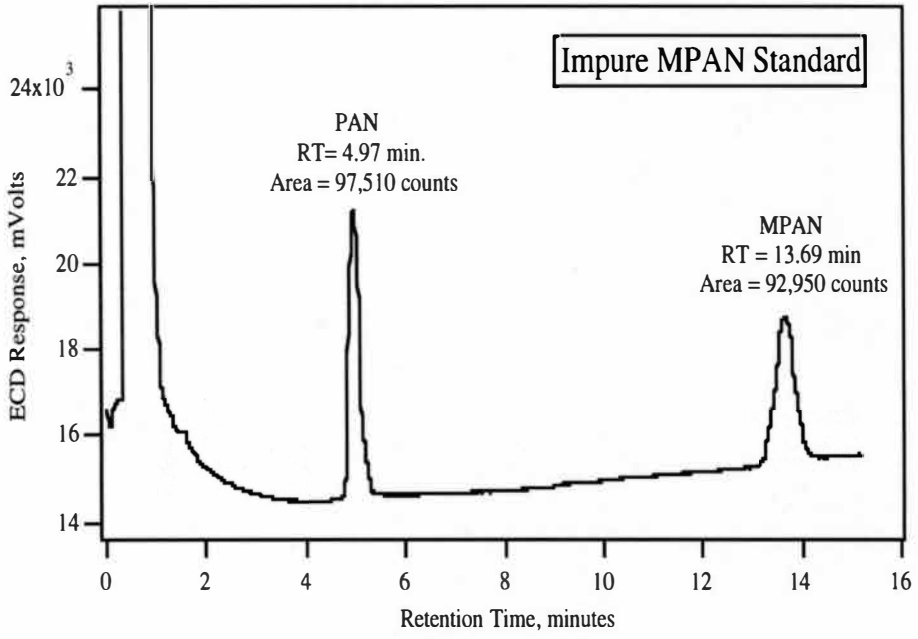

Figure 4. GC/ECD Chromatogram of a Typical Impure MPAN Standard.

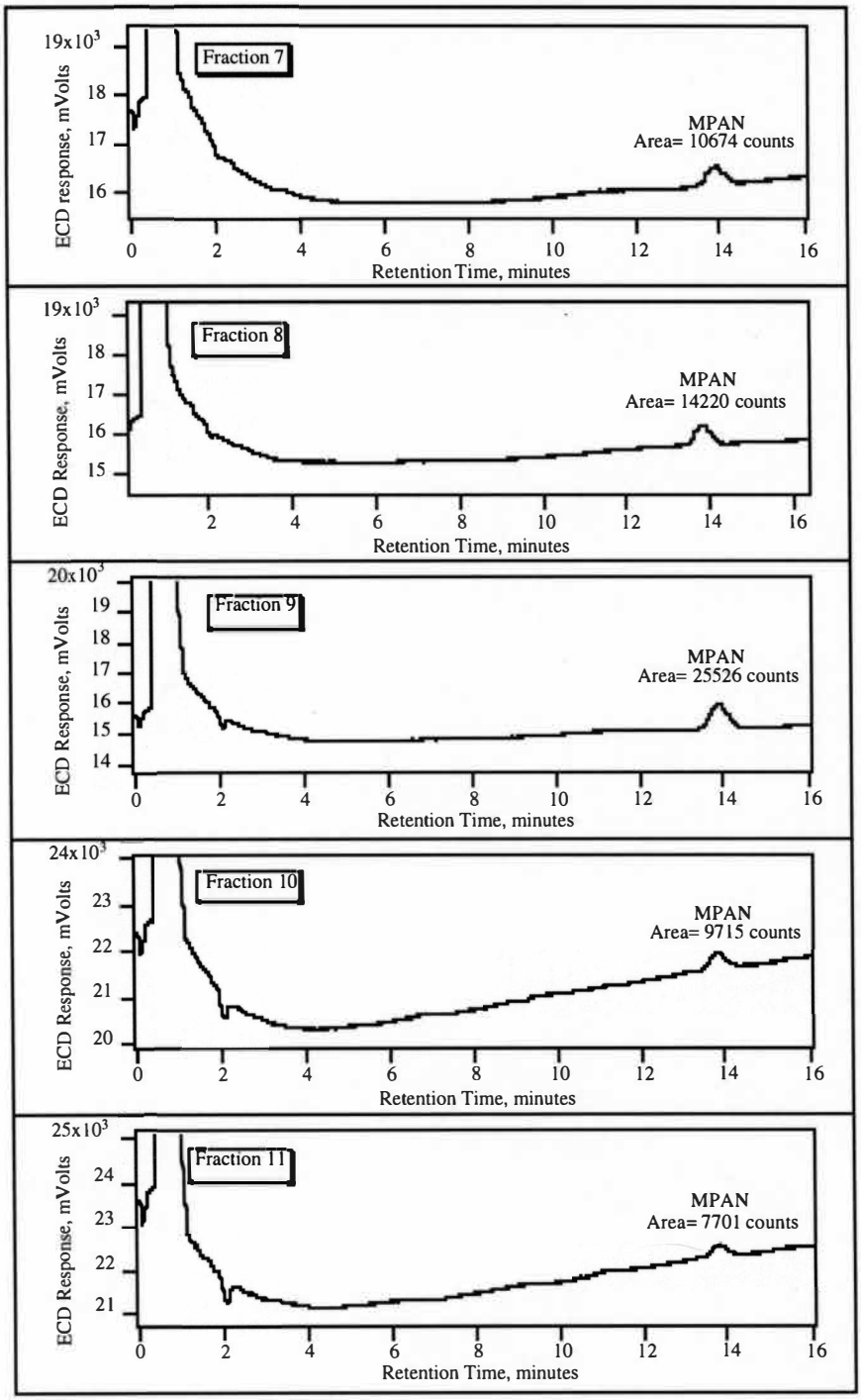

Figure 5. GC/ECD Chromatograms of Different MPAN Fractions Belonging to a Particular MPAN Purification Procedure.

CHAPTER III

RESULTS

General Statistics

Table 2 and Table 3 contains the minima, maxima, means and medians of the compounds and ratios of compounds obtained at the Youth Inc. site for all the data, and the data between 7:00 and 18:00 EST respectively. Of the three PANs, PAN had the highest concentration levels with a mean concentration of 485 pptv. The mean PPN concentration was approximately a tenth of the mean PAN concentration at the site and about 1.7 times larger than the mean MPAN concentration. The absolute PAN, PPN and MPAN concentrations and the ratios of PPN/PAN and MPAN/PAN are similar to ground measurements taken by the NOAA Aeronomy Laboratory in 1994 in New Hendersonville, also a semi-rural area located north east of Nashville. The same ratios are also similar to aircraft measurements taken by the same group in 1995 over the Nashville area, although the absolute PAN, PPN and MPAN concentrations are substantially lower at Youth Inc. (Roberts et al., 1997) where higher temperatures close to the surface lead to an increase in thermal decomposition.

In the daytime, PAN made up on average 9.7% of the total oxidized nitrogen species, NOy, while the contribution of PPN and MPAN to NOy amounted to less than 1 % each (Table 3). NOx ($NO+NO_2$) on the other hand constituted approximately 44% of NOy on average. Fahey et al. (1986) report daytime PAN/NOy and NOx/NOy ratios of 15-20% and 20-30% at Niwot Ridge, Colorado, a non-urban site, during the summer of 1984. Similar ratios were also reported by Ridley et al. (1990) for the same

Table 2

General Statistics of Some of the Compounds and Ratios of Compounds Measured at Youth Inc. (All Data Points) - (6/29/95 - 7/26/95)

Compound	Min.	Max.	Mean	Median	# of Points
PAN (pptv)	35	2142	485	403	2158
PPN (pptv)	5	234	50	40	1884
MPAN (pptv)	4	148	30	23	1726
Isoprene (ppbv)	0.012	7.987	1.055	0.754	712
MACR (ppbv)	0.019	1.335	0.290	0.213	724
MVK (ppbv)	0.020	1.751	0.324	0.247	684
O_3 (ppbv)	BDL*	147	49	48	8692
NO_2 (ppbv)	BDL*	27.0	3.0	2.0	4779
NO (ppbv)	BDL*	23.0	0.5	0.1	5859
NOy (ppbv)	1.0	48.5	8.0	6.0	8324
PPN/PAN (%)	1.8	35	9.5	9.3	1884
MPAN/PAN (%)	0.35	25	6.4	5.9	1726
PPN/Propanal (%)	2.3	150	26	20	561
MPAN/MACR (%)	0.62	104	12	10	709
NOx/NOy (%)	BDL*	100	44	42	4779
PAN/NOy (%)	0.34	25	7.3	6.4	2158
PPN/NOy (%)	0.02	2.7	0.72	0.58	1884
MPAN/NOy (%)	0.02	2.4	0.5	0.3	1726

* = Below Detection Limit

Table 3

General Statistics of Some of the Compounds and Ratios of Compounds Measured at Youth Inc. Between 7:00 and 18:00 EST - (6/29/95 - 7/26/95)

Compound	Minimum	Maximum	Mean	Median	# of points
PAN (pptv)	35	2142	639	584	1075
PPN (pptv)	6	324	63	52	991
MPAN (pptv)	4	148	35	29	942
Isoprene (ppbv)	0.014	5.015	1.207	1.050	380
MACR (ppbv)	0.019	1.182	0.267	0.214	371
MVK (ppbv)	0.020	1.751	0.325	0.269	364
O_3 (ppbv)	BDL*	138	60	61	4278
NO_2 (ppbv)	BDL	27.0	2.5	1.5	2303
NO (ppbv)	BDL*	21.2	0.7	0.2	3402
NOy (ppbv)	1.0	48.5	7.5	5.5	3955
PPN/PAN (%)	2.5	28	9.5	9.3	1030
MPAN/PAN (%)	0.40	21	6.1	5.6	961
PPN/Propanal (%)	2.3	150	29	23	319
MPAN/MACR (%)	2.1	104	15	12	356
NOx/NOy (%)	1.1	99	36	30	2303
PAN/NOy (%)	0.34	25	9.7	9.9	1075
PPN/NOy (%)	0.052	2.7	0.91	0.81	1030
MPAN/NOy (%)	0.020	2.4	0.55	0.47	961

* = Below Detection Limit

site in 1987. Parrish et al. (1993) report median daytime PAN/NOy and NOx/NOy ratios of 12-25% and 25-40% respectively for six rural sites in Eastern North America. The higher NOx/NOy and lower PAN/NOy ratios at Youth, Inc. compared to Niwot Ridge and the other rural sites is due to the closeness of Youth, Inc. to pollution sources where the air is relatively unprocessed by the time it reaches the site.

The median ratio of MPAN/MACR was roughly half that of PPN/Propanal. Thermal decomposition is expected to be the main loss process for MPAN and PPN which have similar formation routes from MACR and propanal respectively. However in the case of MACR, OH radicals may equally abstract a hydrogen to form MPAN, in a manner similar to hydrogen abstraction from propanal, or add to the double bond in 1:1 ratio (Tuazon and Atkinson, 1990a) which explains the difference between the two observed percent ratios since there are no unsaturation sites on propanal for OH to add to.

The isoprene and MACR maxima (Table 2) are relatively similar to the maxima reported by Biesenthal et al. (1997b) for a site in the Lower Fraser Valley, Bristish Columbia which is influenced like Youth, Inc. by both biogenic emissions and anthropogenic emissions from the city of Vancouver. Higher isoprene and MACR concentrations have been reported for more rural and forested areas (Martin et al., 1991; Montzka et al., 1993).

PAN, PPN, MPAN and O_3 Diurnal Observations

The mean diurnal cycles of PAN, PPN, MPAN and ozone (Figure 6) at Youth Inc. are typical of open flat terrain, where the three PANs experience a sharp daily increase in the morning, peak around noon and finally start decreasing as the day progresses into night (Parrish et al., 1993). The morning rise in the three PANs and

ozone coincides early in the morning with the breakup of the nocturnal boundary layer (NBL) which mixes relatively high concentrations from the residual layer aloft. Photochemical production of PANs takes over as the solar flux increases and induces the production of hydroxyl radicals which drive the daytime chemistry of the troposphere. In the afternoon, the concentrations of PAN compounds begin to decrease due to an increase in the concentration of OH radicals which are solar flux

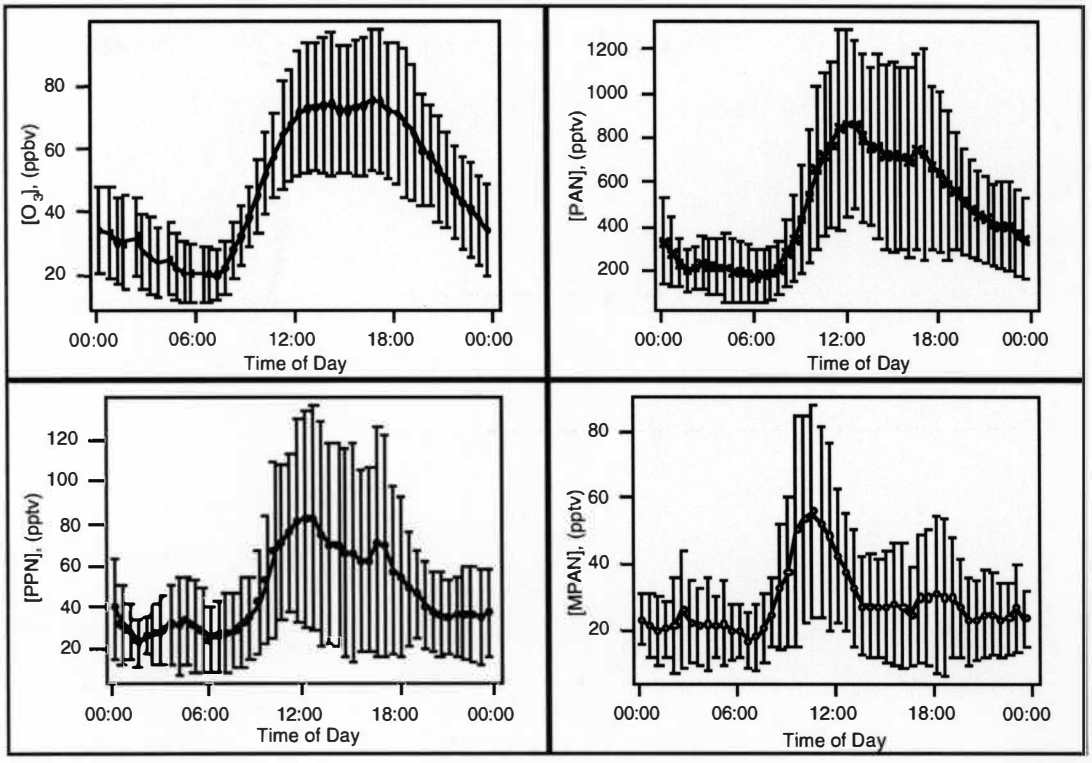

Figure 6. Mean Diurnal Plots of PAN, PPN, MPAN and Ozone With Their Standard Deviations at 1/2 Hour Intervals.

dependent, an increase in temperature and a decrease in hydrocarbon precursors. At night, the photochemical production of PAN compounds comes to a halt as hydroxyl radicals are only available during the day. The NBL forms at night, traps the air close to the surface, and prevents PAN compounds from above the NBL to mix with the air

below. Hence without any production or mixing, the PAN compounds below the NBL begin to undergo surface deposition (Garland and Penkett, 1976; Shepson et al., 1992a; Schrimpf et al., 1996) and their concentrations decrease exponentially until the NBL breaks up again in the morning and the cycle is repeated.

MPAN appears to be shorter lived in the daytime relative to PAN, PPN and ozone. On average, the MPAN levels peak around 10:30 and quickly drop afterward. PAN and PPN peak at 12:00 and 12:30 respectively, but unlike MPAN, their concentrations persist longer through the late afternoon and their diurnal cycles resemble that of ozone more so than MPAN. The apparently shorter lifetime of MPAN, which may be in part due to the susceptibility of MPAN's double bond to attack by ozone and hydroxyl radicals, and its dependence on a single biogenic precursor, MACR, may make MPAN more sensitive than either PAN or PPN to local biogenic photo activity.

There are days however when the mean diurnal trend for PAN, PPN and MPAN is not followed and when the site is dominated by either anthropogenic or biogenic regimes. July 19, for example, is a day that is dominated by air richer in anthropogenic VOCs that was transported to the site (Figure 7). The late afternoon peaks in PAN and PPN indicate transport from a region with high levels of anthropogenic pollution. PAN and PPN tracked well throughout the day and gradually increased and peaked around 17:00 EST. MPAN remained low throughout that day even when PAN and PPN peaked in the late afternoon. On the hand, July 17 was a day that witnessed high levels of the biogenic compound MPAN that occasionally exceeded the concentrations of PPN, unlike the average diurnal trend. However, all three PAN compounds had high concentrations and tracked throughout the day. The effects of anthropogenic chemistry seen through PPN were still significant since

anthropogenic precursors originate and are advected toward the site along with NO_x which is needed to synthesize the biogenic compound MPAN.

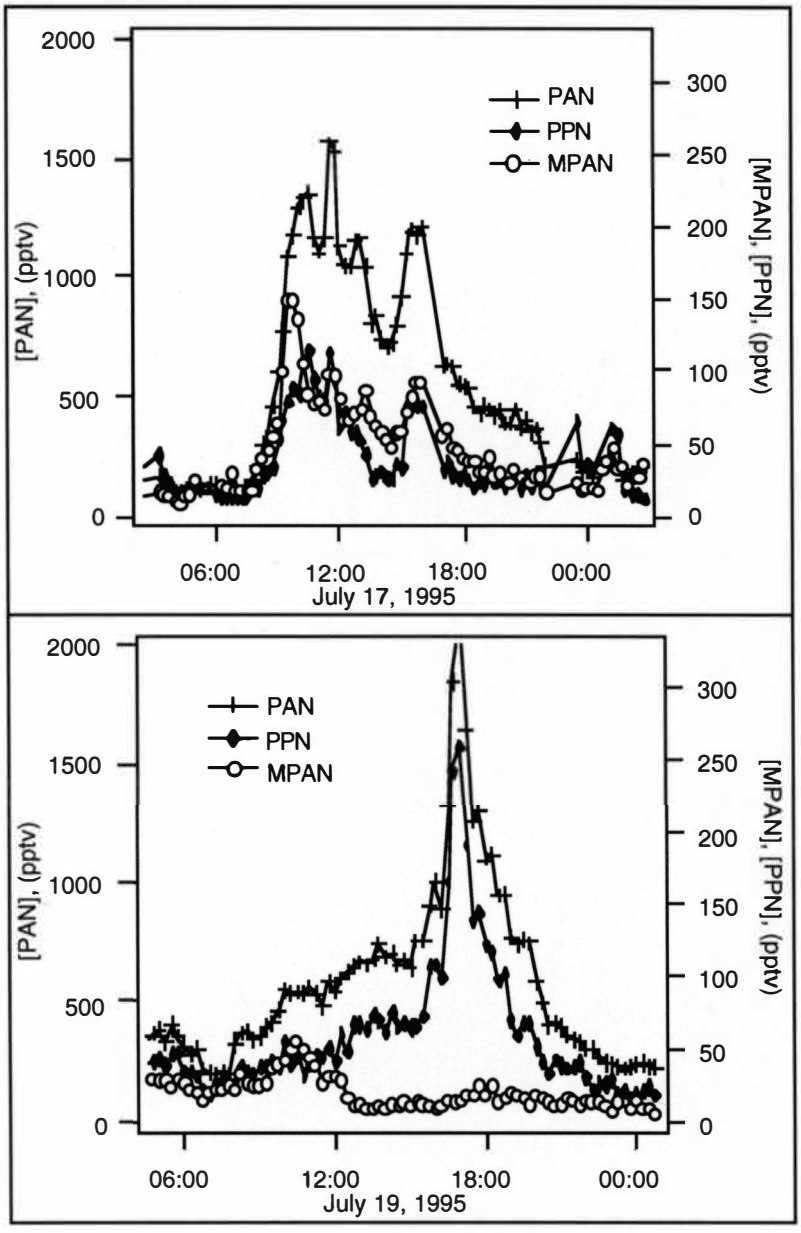

Figure 7. Time Series Examples of PAN, PPN and MPAN Not Following Their Mean Diurnal Trends.

The mean diurnal concentrations of MPAN, MACR and isoprene are shown in Figure 8. Daytime MPAN levels appear to be dependent on the availability of its precursor MACR which MPAN closely tracks with a slight delay. The daytime MPAN-MACR tracking suggests that MACR is produced at least as fast as MPAN is produced. After 18:00 EST, the tracking between MPAN and MACR is not as good as during the day. Without OH radicals, MPAN production slows considerably at night while MACR can still be produced from the reaction of isoprene with ozone or can be transported to the site along with isoprene. PPN and propanal show a similar daytime trend; however, they decrease at a slower rate in the afternoon (Figure 9).

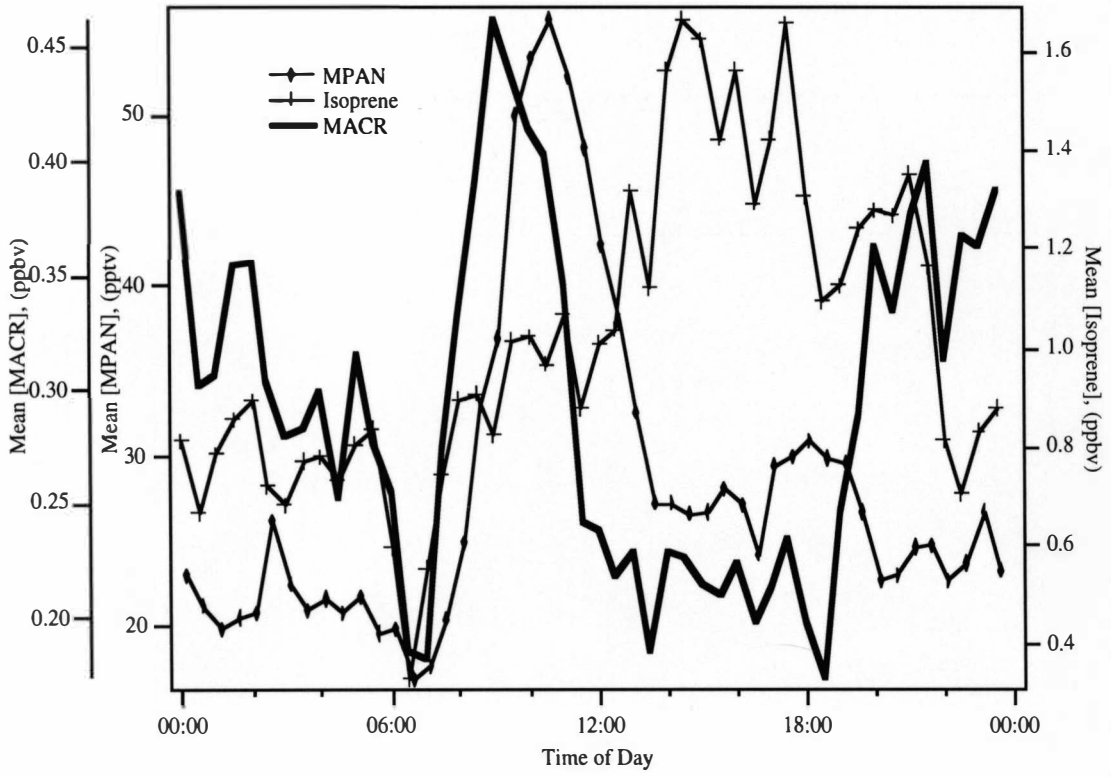

Figure 8. Mean Diurnal Plots of Isoprene, MACR and MPAN at 1/2 Hour Intervals.

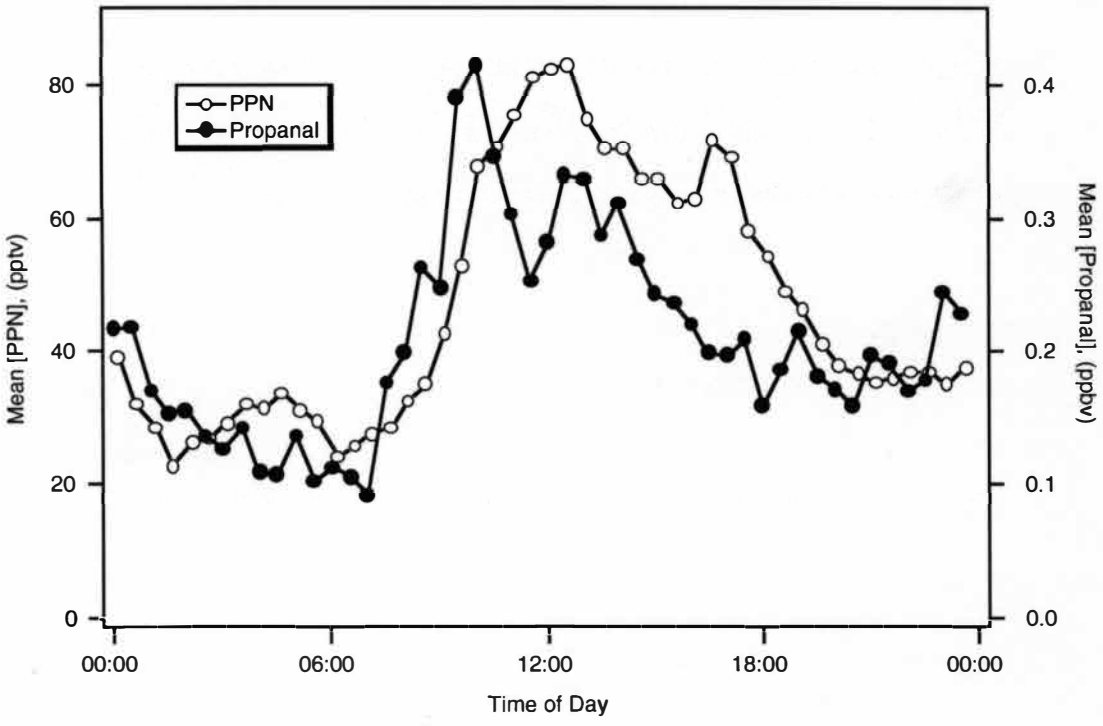

Figure 9. Mean Diurnal Plots of PPN and Propanal at Half-Hour Intervals.

The sharp morning peak in MACR concentration does not appear to be dependent on isoprene which typically peaks toward mid-afternoon. This is an indication that MACR may be introduced in the morning by the break up of the NBL rather than by isoprene photooxidation alone. One way to examine this is to look at the mean diurnal plot of the methyl vinyl ketone (MVK) to methacrolein ratio for the entire sampling period (Figure 10). The MVK/MACR ratios due to the reaction of isoprene with ozone and hydroxyl radicals are 0.4 and 1.4 respectively (Aschman and Atkinson, 1994). The reaction of isoprene with OH radicals is the dominant loss process of isoprene during the day and hence a ratio of about 1.4 would be expected. Isoprene ozonolysis takes over at night and the MVK/MACR ratio should be equal 0.4 but never quite reaches this level due to the presence of MVK and MACR produced during the day from OH chemistry. Between midnight and 9:30 EST, the average of the

MVK/MACR ratios in Figure 10 is equal to 0.85 ± 0.08 and this ratio does not begin to change until around 10:00 EST, long after the NBL breaks up. Due to the absence of surface deposition above the NBL, ozone levels may be high enough to react with isoprene to produce reasonable amounts of MVK and MACR. Since the MVK/MACR ratio does not vary much before and after the NBL breaks up, it can be inferred that the morning rise in MACR is due to the break up of the NBL and not solely due to OH reaction with isoprene in the early morning. The MVK/MACR ratio typical of OH+isoprene reaction is not reached until noon and remains steady into the early evening hours. The MVK/MACR average between 12:00 and 19:30 EST was 1.39 ± 0.10. After 20:00 EST, this ratio begins to drop again as the ozone+isoprene reaction becomes significant.

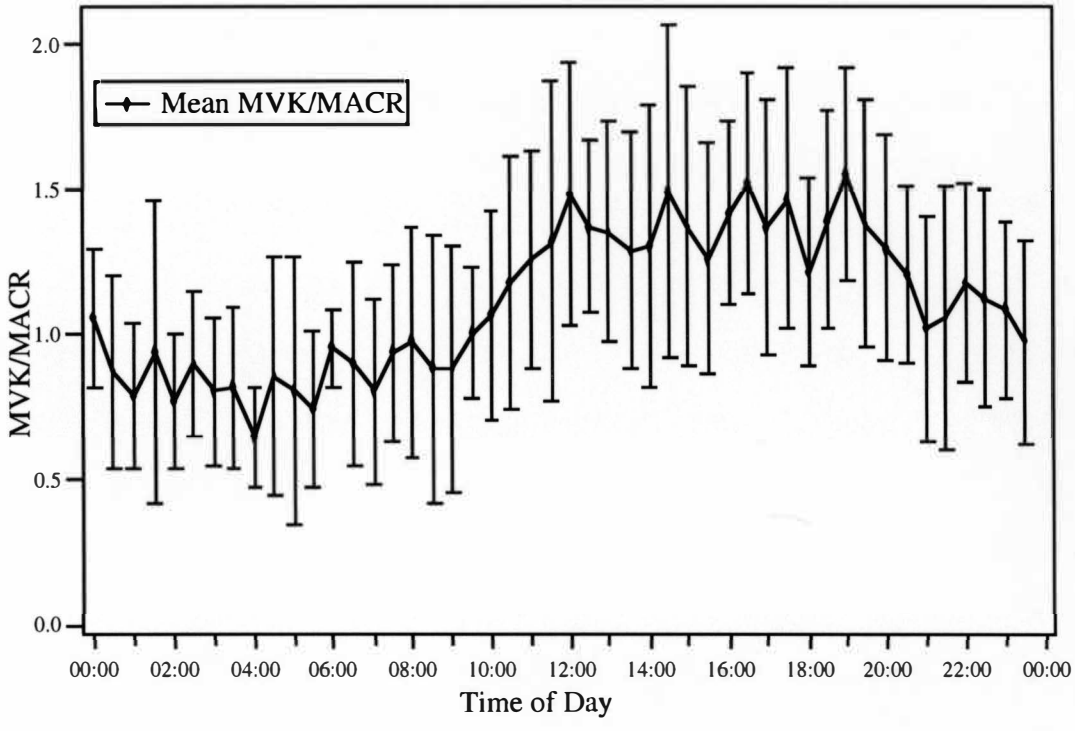

Figure 10. Mean Diurnal Plot of MVK/MACR With Standard Deviations at 1/2 Hour Intervals.

Similarly, it can be inferred that MPAN is also introduced from the air layer above the NBL because PANs above the NBL would be expected to be relatively more stable due to higher NO_2/NO ratios, lower temperatures, and absence of surface deposition which increase PAN lifetime. In a NO_x rich environment such as in the Nashville area, it is possible that MPAN production from NO_3 radical chemistry may also occur above the NBL. Starn et al. (1997a) provide evidence for the nighttime production of MPAN at Youth Inc. from the reaction of NO_3 radicals with MACR. If the morning increase in MACR and MPAN were only due to fresh OH radical chemistry, the MVK/MACR ratio would have rapidly increased in the morning to 1.4.

Nevertheless, photochemical production of MPAN also occurs in the morning. The observed lagging between MPAN and MACR especially around late morning might be due to OH photochemical MPAN production. The rate of MPAN formation should be proportional to the product of $k*\beta*[MACR]*[OH]$ where k is the rate constant and β is the fraction of hydrogen abstraction from MACR. Since [OH] is difficult to measure directly (The 1993 Tropospheric OH Photochemistry Experiment, 1997) and no effort was made to measure it at Youth Inc., the rate of OH formation was qualitatively estimated and used as a surrogate for [OH]. The rate of OH formation was qualitatively calculated from ozone photolysis at 308 nm using ambient measurements of O_3, temperature, relative humidity, pressure, and total solar flux (see Appendix A). Figure 11 shows MPAN and the product of [MACR] * (OH formation rate at 308 nm) peaking on average at the same time in the morning which indicates that photochemical production occurs in the morning. The dip in MPAN that is seen in the afternoon relative to [MACR] * (OH formation rate) is due to a decrease in MPAN lifetime.

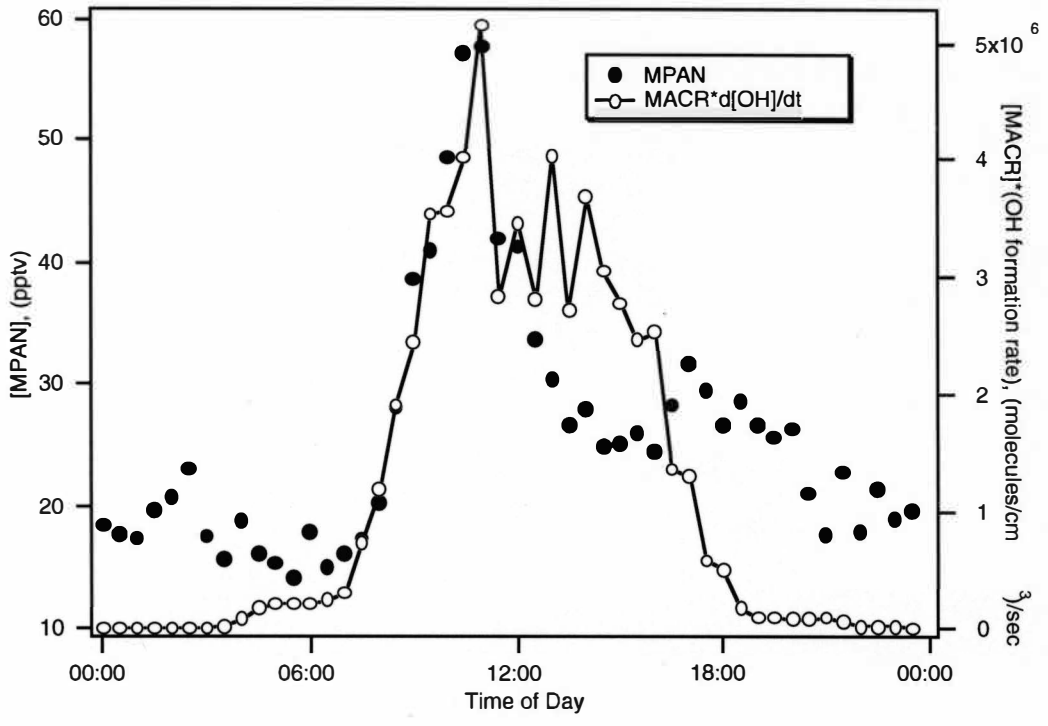

Figure 11. Mean Diurnal Plots of MPAN and the Product of MACR and OH Formation Rate at 308 nm at 1/2 Hour Intervals.

PPN and MPAN Versus PAN

Figure 12 is a plot of PPN and MPAN versus PAN. There is a direct linear correlation (R^2 = 0.76) between PAN and PPN, which appears to deviate at high concentrations to a higher slope. The increase in slope at higher concentrations has been attributed by Singh and Salas (1989) to more efficient PPN production from precursors such as 1-butene which are prevalent in urban areas and have relatively shorter lifetimes than PAN precursors such as n-butane. As the distance from urban areas increases, less PPN precursors will be available and the slope will become smaller along with absolute concentrations. The PPN and PAN data used by Singh and Salas were compiled from a number of measurement campaigns and plotted together on one graph which clearly showed an exponential relationship. In the case of

MPAN versus PAN, a less clear correlation is evident as confirmed by linear regression analysis ($R^2 = 0.29$), although there is a clear upper bound. The weaker correlation between MPAN and PAN might be caused in part by the shorter diurnal cycle of MPAN with respect to that of PAN and PPN. Another plausible explanation may be that more PAN might be produced at Youth Inc. from anthropogenic hydrocarbons than from isoprene photooxidation and hence a better correlation between PPN and PAN.

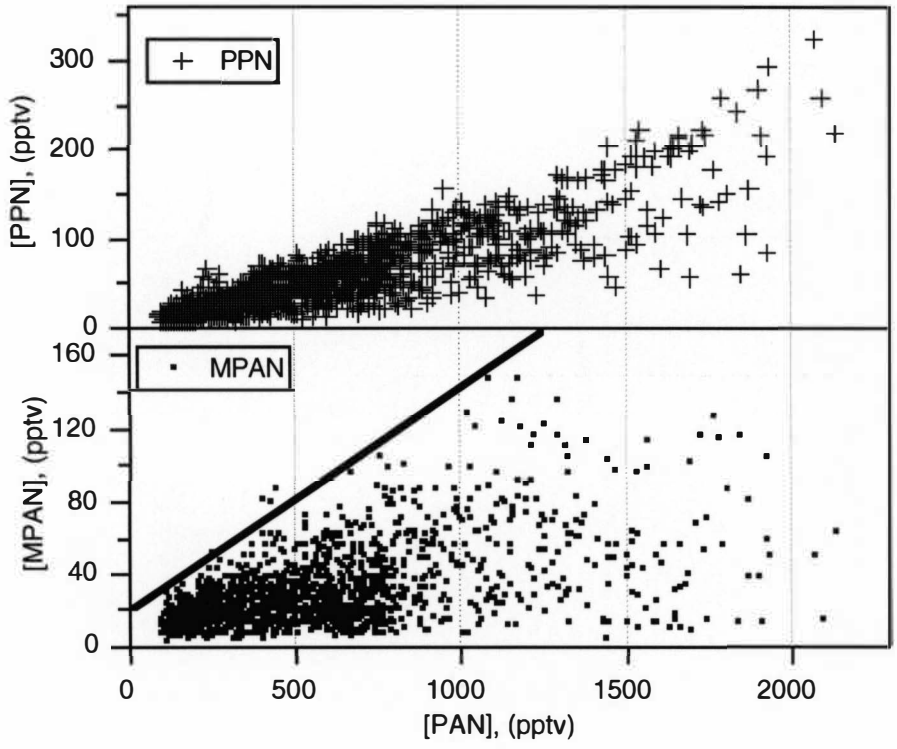

Figure 12. PPN and MPAN Versus PAN for the Entire Sampling Period.

Peroxyacyl Nitrates Versus Ozone

Scatter plots of each of PAN, PPN and MPAN versus ozone are shown in Figure 13. Linear fits show that O_3 correlates best with PAN, followed by PPN and then MPAN. The poor correlation between ozone and MPAN may be due to the

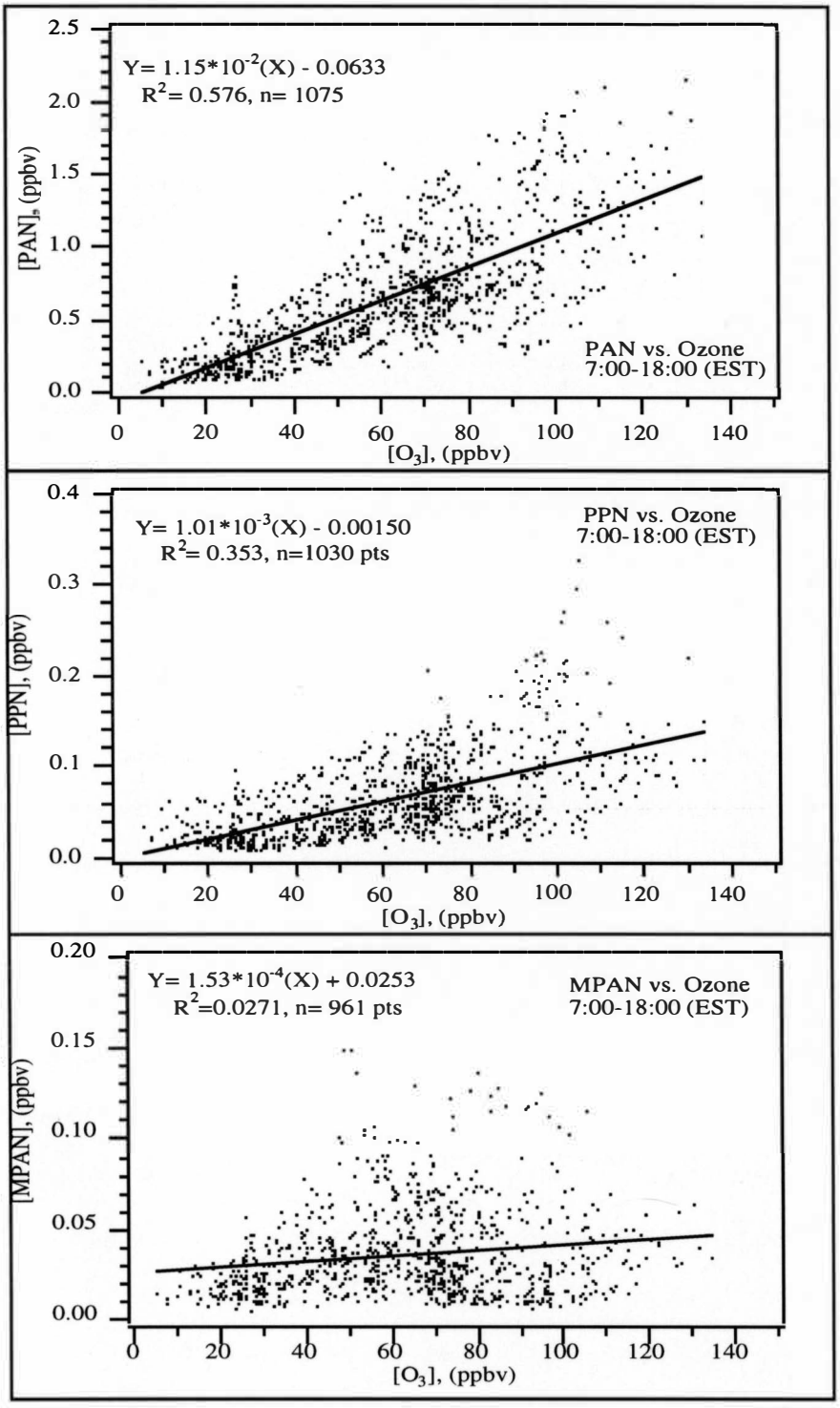

Figure 13. PAN, PPN and MPAN Versus Ozone Between 7:00 and 18:00 EST for the Entire Sampling Period.

difference in their ambient lifetimes. What is interesting about the PAN/O_3 slope at Youth Inc. is that it is smaller than the PAN/O_3 slope of 0.0242 for the daytime data of a number of combined North American rural sites (Roberts et al., 1995) despite the proximity of Youth Inc. to urban areas. The PAN/O_3 slope is normally greater in urban areas than in rural areas, and gradually decreases as urban masses move away towards rural areas (Shepson et al., 1992b; Sirois and Bottenheim, 1995). For instance, PAN/O_3 slopes of 0.039 and 0.048 have been reported by Ridley et al. (1990) between the hours of 10:00-17:00 MDT for polluted air masses at Boulder and Niwot Ridge, Colorado and are 3.4 and 4.2 times larger than the slope measured at Youth Inc. respectively. Due to the closeness of the Youth Inc. Ranch to the city of Nashville, a larger PAN/O_3 slope would be expected.

One plausible explanation for the smaller PAN/O3 slope at Youth Inc. is the possibility that isoprene photooxidation may be more efficient in forming ozone than PAN, but this needs to be substantiated with further studies. Although the slope reported by Roberts et al. is for the combined daytime data of four sites, a qualitative calculation of the daytime PAN/O_3 slope for each site was done using the average daytime plots of PAN versus ozone for each site in the Roberts et al. paper. The Scotia, Pennsylvania site was found to have the smallest PAN/O_3 slope followed by the Whitetop Mountain, Virginia site. The Scotia data were collected in an oak forest environment which is a major source of isoprene and hence is similar to the Youth Inc. environment. The Whitetop Mountain site, a high elevation site, was surrounded by spruce trees which eventually blended with birch trees further down from the site. In contrast, the sites in Egbert, Ontario and Bondville, Illinois had higher estimated PAN/O_3 slopes and were located in flat agricultural areas which could possibly be producing less isoprene than the forested sites.

In a setting similar to Youth Inc., a PAN/O_3 slope of 0.017 was reported for the Delft, Netherlands area (Nieboer and van Ham, 1976), which is also smaller than the slope reported by Roberts et al. for the rural sites. During the Delft campaign, the wind blew more than 50% of the time from a relatively rural area sector containing partly heated greenhouses, which could contribute both nitrogen oxides and biogenic hydrocarbons. Hence, it is conceivable that isoprene may be more efficient in forming ozone than in forming PAN which would justify the lower slope at the Youth Inc. Ranch.

Relationship of Peroxyacyl Nitrates With NOy

The term NOy refers to the sum of oxidized nitrogen species in the atmosphere. It includes NOx, HNO_3, HONO, PANs, alkyl nitrates and particulate nitrates (inorganic). An unprocessed air mass consists mainly of NOx. As air masses age photochemically, the percentage of NOx/NOy decreases since NOx becomes processed into other forms such as PANs and HNO_3 and the percentage of PANs/NOy and HNO_3/NOy increases. The mean diurnal plots of PAN/NOy, PPN/NOy and MPAN/NOy (Figure 14) show a pattern similar to the mean diurnal plots of PAN, PPN and MPAN. A simultaneous increase in PAN compounds and the ratio of PAN compounds to NOy is a sign of air mass aging due to fast photochemistry which converts NOx to PANs. Based on Figure 14 and Table 2, only PAN and NOx constitute a significant amount of NOy, while the contribution of PPN and MPAN to NOy is significantly less. HNO_3 should also make up a significant portion of NOy (Williams et al., 1997a; Parrish et al., 1993; Fahey et al., 1986), but HNO_3 measurements were not taken at Youth, Inc.. The fact that MPAN constituted a small fraction of NOy during the day and that its ambient lifetime is shorter compared to PAN

indicates that MPAN may not be an important sink of NOx at the Youth Inc. site and its contribution to ozone formation may be limited to local production.

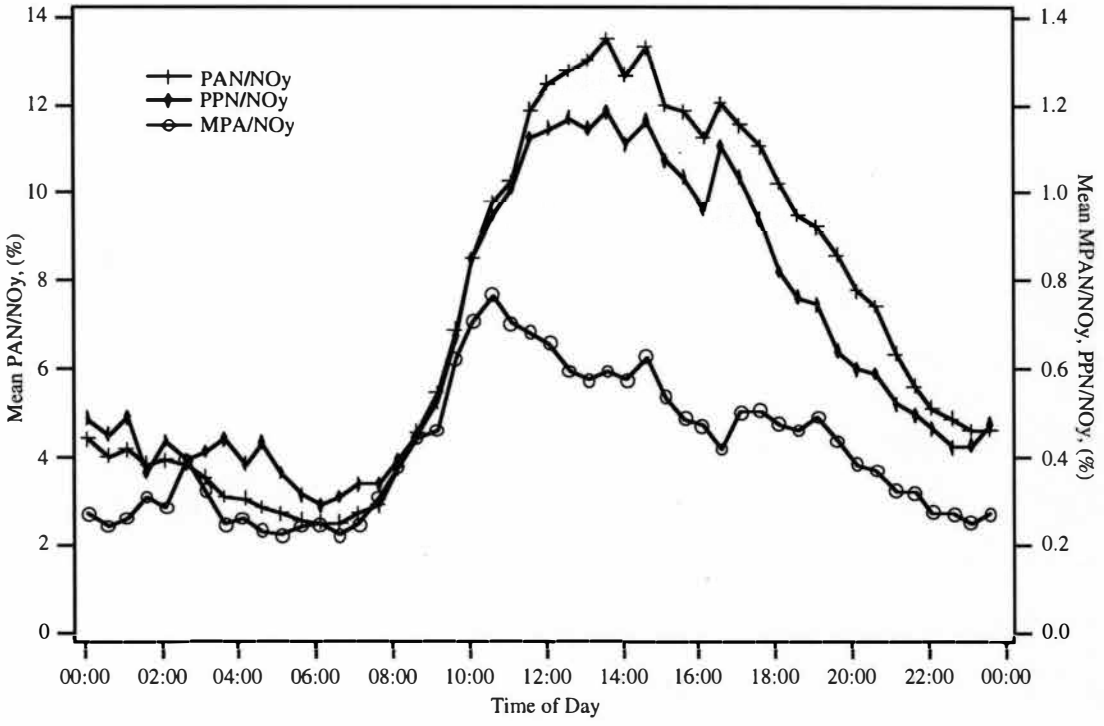

Figure 14. Mean Diurnal Plots of PAN/NOy, PPN/NOy and MPAN/NOy at 1/2 Hour Intervals.

CHAPTER IV

DISCUSSION

Systematic Relationship Between MPAN and MACR

While they are in general representative of most of the data, diurnal averages may hide important and interesting events. For instance while the diurnal patterns in Figure 8 show MPAN and MACR tracking well, on certain days like July 17 MPAN and MACR do not track each other (Figure 15). A linear fit for MPAN versus MACR for July 17 during the daytime gave a poor correlation, R^2= 0.01 (Figure 16). The equation of the fit was $[MPAN]_{(pptv)} = -25.1*[MACR]_{(ppbv)} + 67.9$ for a total of 21 points. In contrast, July 19 is a day when MPAN closely tracks MACR (Figure 15) and a plot of MPAN vs. MACR for 17 daytime points (Figure 16) provided a reasonably good correlation (R=0.71) with an equation of $[MPAN]_{(pptv)} = 179.7*[MACR]_{(ppbv)} + 0.5$.

In order to try to understand why MACR and MPAN at times correlate and at other times do not, the following approach was taken. Daily MPAN versus MACR plots were made for daytime data between the hours of 7:00 and 18:00 EST. The choice of the daytime range of 7:00-18:00 was based on the mean diurnal solar flux plot at Youth Inc. where the solar flux began to increase around 5:00 EST and approached zero around 20:00 EST. The time range of 7:00-18:00 EST ensures that all daytime MPAN-MACR observations are made during periods suitable for OH photochemistry. The correlation factor, R, for each day was then used to group the days into distinct categories. Based on the histogram in Figure 17, three groups of days

were distinguished: (1) 6 days when R<0.1, (2) 4 days when 0.3<R<0.6 and (3) 12 days when R>0.6. The goal was to investigate whether the relationship between MPAN and MACR reflects features of chemistry by looking for trends in the levels of different compounds and ratios of compounds that are related to MPAN and MACR chemistry.

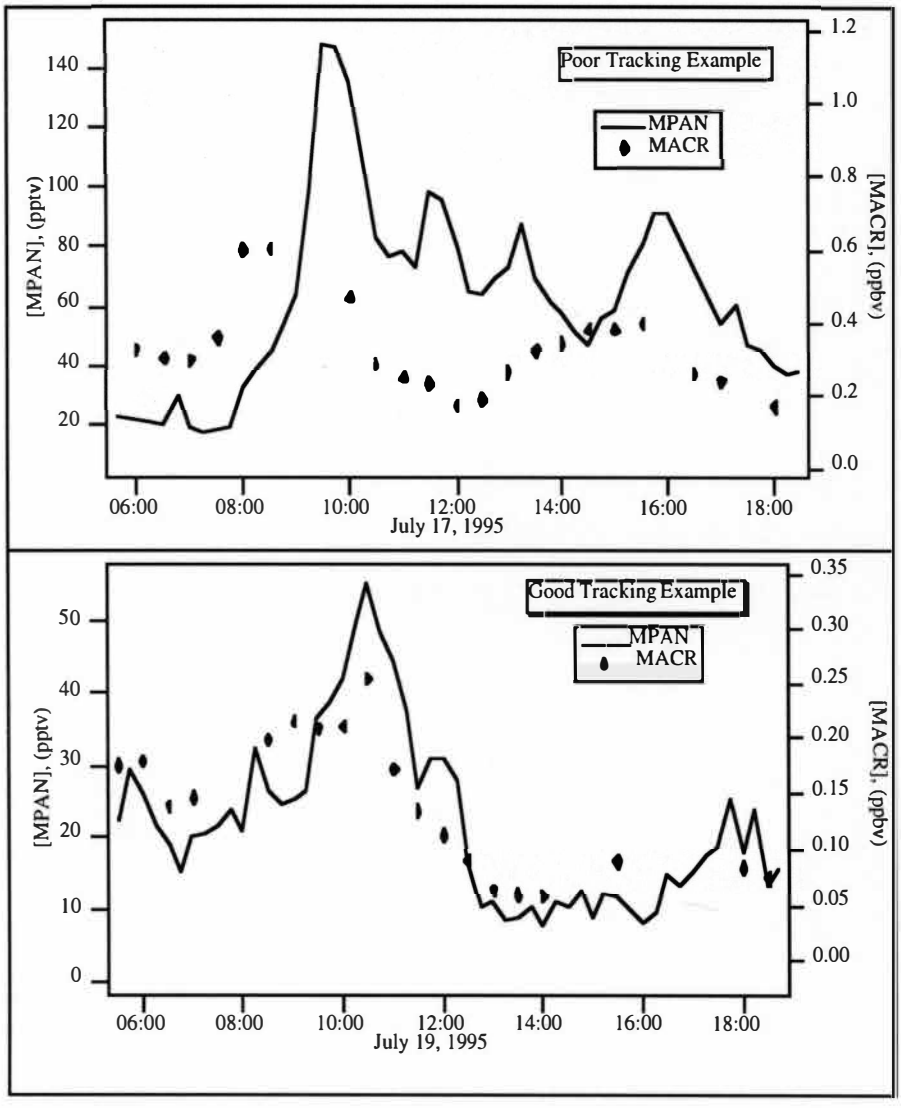

Figure 15. MPAN and MACR Time Series Plots for July 17 and July 19 Showing Poor and Good Tracking Respectively Between the Two Compounds.

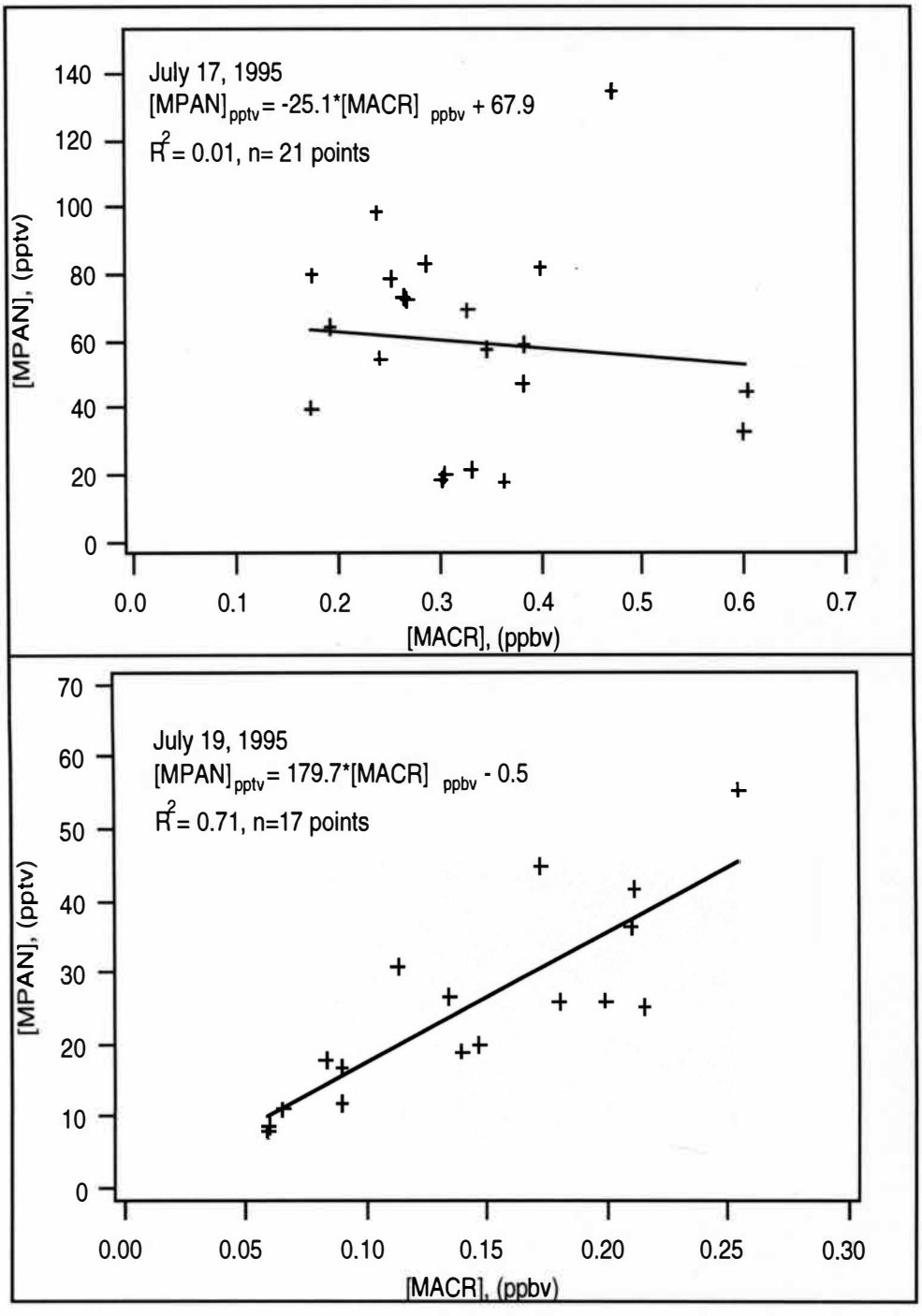

Figure 16. MPAN Versus MACR Between 7:00-18:00 EST on July 17 and July 19, 1995.

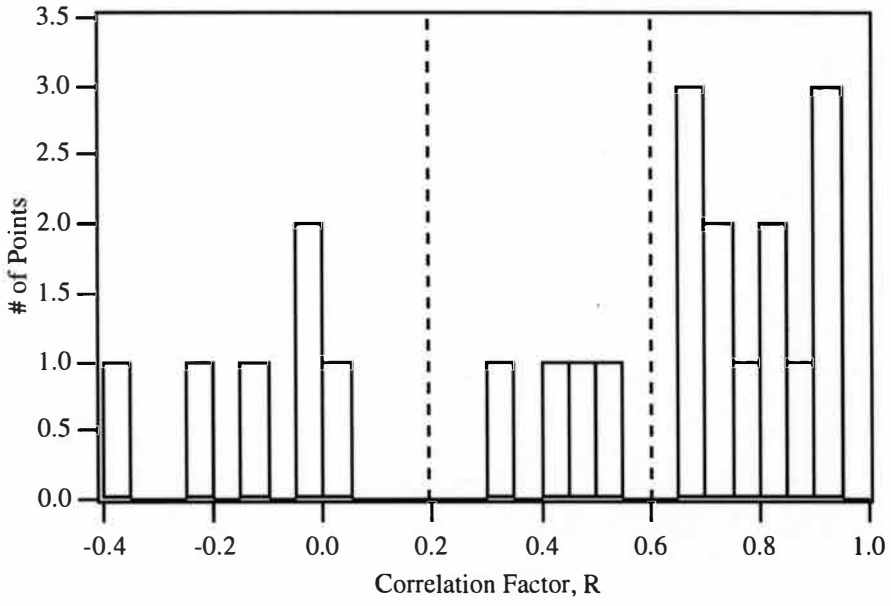

Figure 17. Histogram of Correlation Factors Obtained From Daily MPAN Versus MACR Fits.

Based on median values, a significant trend could not be seen for each of MPAN, MACR, isoprene, ozone and OH formation rate with an increase in MPAN-MACR correlation. There appeared to be however a direct relationship between MPAN and OH formation rate (Figure 18) which is reasonable since the formation of MPAN is dependent on the availability of hydroxyl radicals. The most striking feature in this analysis is the absolute NO_2 median concentration during periods of low MPAN-MACR tracking which is about a factor of 2 larger than the times when MPAN and MACR track well (Figure 19). This suggests that NO_x has a role in controlling the behavior between MPAN and MACR. High levels of NO_2 effectively sink OH radicals and hence interfere with isoprene photochemistry. The wind direction data (Figure 20), filtered for wind velocities of 2 m/s or greater, reveals that air masses impacted the site only from the west (slightly NW) and south (slightly SW) during days with low MPAN-MACR correlation ($R<0.1$ range). These two wind directions point toward

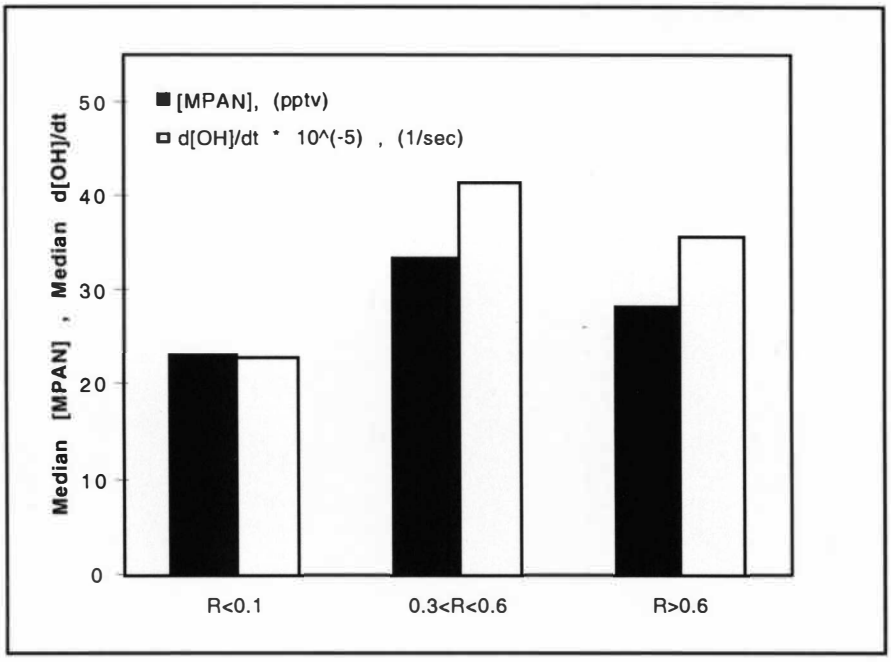

Figure 18. Median MPAN and OH Formation Rate at 308 nm Values for the Three Types of Days, Based on the Correlation Between MPAN and MACR.

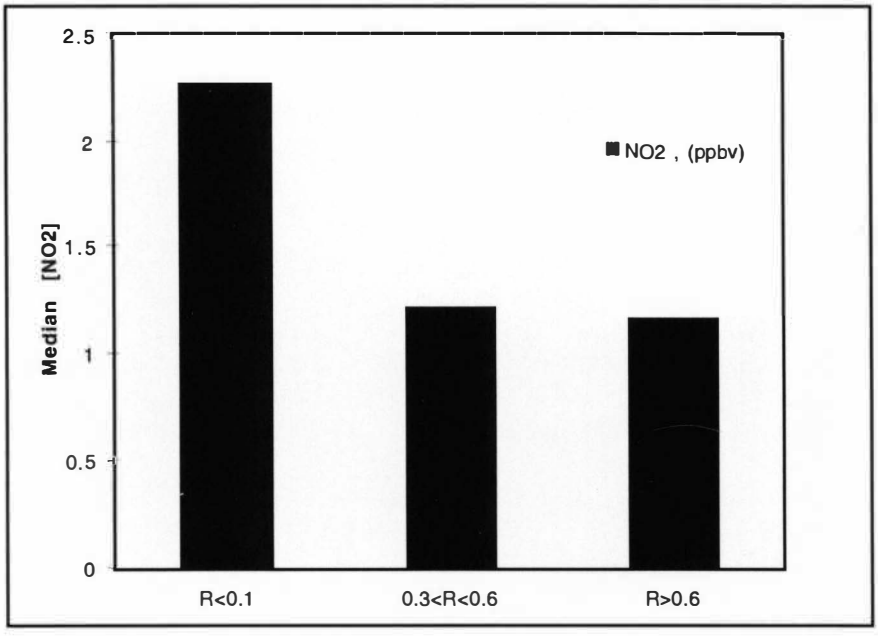

Figure 19. Median NO_2 Concentrations for the Three Types of Days, Based on the Correlation Between MPAN and MACR.

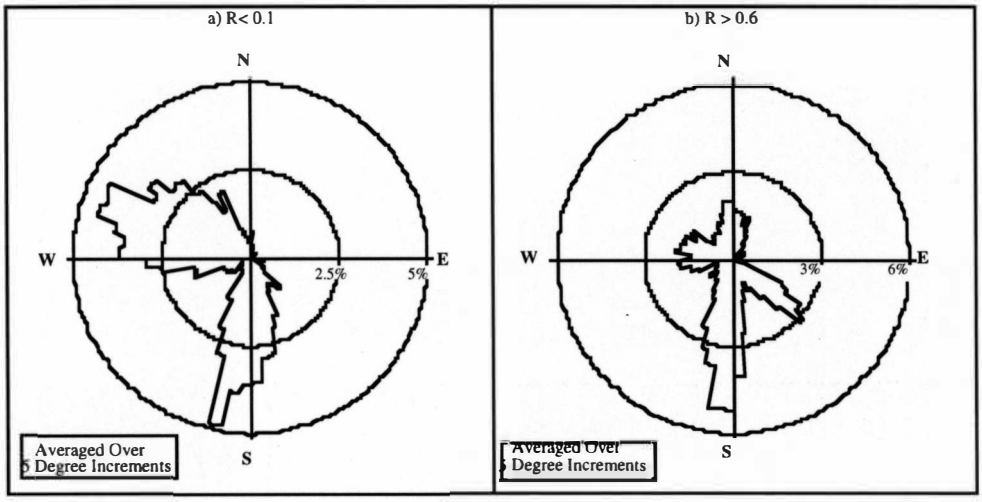

Figure 20. Wind Rose Plots Showing the Average Percent Distribution of the Wind Direction Data at 5 Degree Increments for Days When MPAN and MACR Were a) Poorly (R<0.1) and b) Well Correlated (R>0.6).

areas which are likely to provide significant anthropogenic influences, especially the western direction where the Nashville area is located. This finding is in agreement with the higher NO_2 levels seen for days with low tracking between MPAN and MACR. For the periods of high MPAN-MACR tracking (R>0.6), air impacted the site primarily from the south and southeast.

The thermal lifetime of PANs increases with the ratio NO_2/NO. PANs thermally decompose into NO_2 and peroxyacyl radicals. NO_2 and NO compete for the peroxyacyl radicals to reform PANs or to decompose the peroxyacyl radicals respectively. Hence at higher NO_2 concentrations relative to NO, less PANs will decompose and their thermal lifetimes will be longer. The NO_2/NO medians for the different categories were found to be similar at 9.62, 8.15 and 10.7 respectively which would indicate that the thermal lifetime of MPAN is quite similar in all three periods suggesting that OH and O_3 affect MPAN lifetime and the tracking between MPAN and MACR. Since the time span of 7:00-18:00 EST for this analysis is fairly long, it is

possible that important episodes where NO_2/NO might be critical to MPAN lifetime could have been masked by the rest of the time period.

Case Studies of MPAN-MACR Correlation and Non-Correlation

Since the analysis in the previous section is general and qualitative in nature, there is potential for information loss when looking at the medians of different compounds for a number days within the time period of 0700 hours to 1800 hours. More attention will be focused in this section on analyzing events of specific days when MPAN either tracked or did not track MACR. July 17 and 19 are good examples of days when MPAN and MACR were non-correlated and correlated respectively. Figures 21 and 22 are plots of MPAN, MACR, NO_2/NO, solar flux and temperature for July 17 and 19 respectively. It is important to note that TVA's final data set did not contain any NO_2 and NO_2/NO data for July 17, 1995, and therefore it was necessary to resort for both days to the preliminary data sets in which the accuracy of the data was uncertain (K. Olszyna, personal communication).

On July 17, the morning was sunny and warm, and the afternoon was characterized by lower solar flux and temperatures caused by clouds and a thunderstorm. There are two periods after the morning peak where there is a deviation in the correlation between MPAN and MACR. At about 11:00, a sharp increase in NO_2/NO during a photochemically active part of the day causes a simultaneous increase in MPAN which lasts approximately one hour. Then the tracking between MPAN and MACR resumes temporarily until approximately 13:15 when overcast conditions cause a drop in OH production. This limits the rate of conversion of MACR to MPAN despite the abundance of MACR. Between 1430 and 1600 hours, MPAN increases again as air with higher NO_2/NO and lower temperature impacts the site.

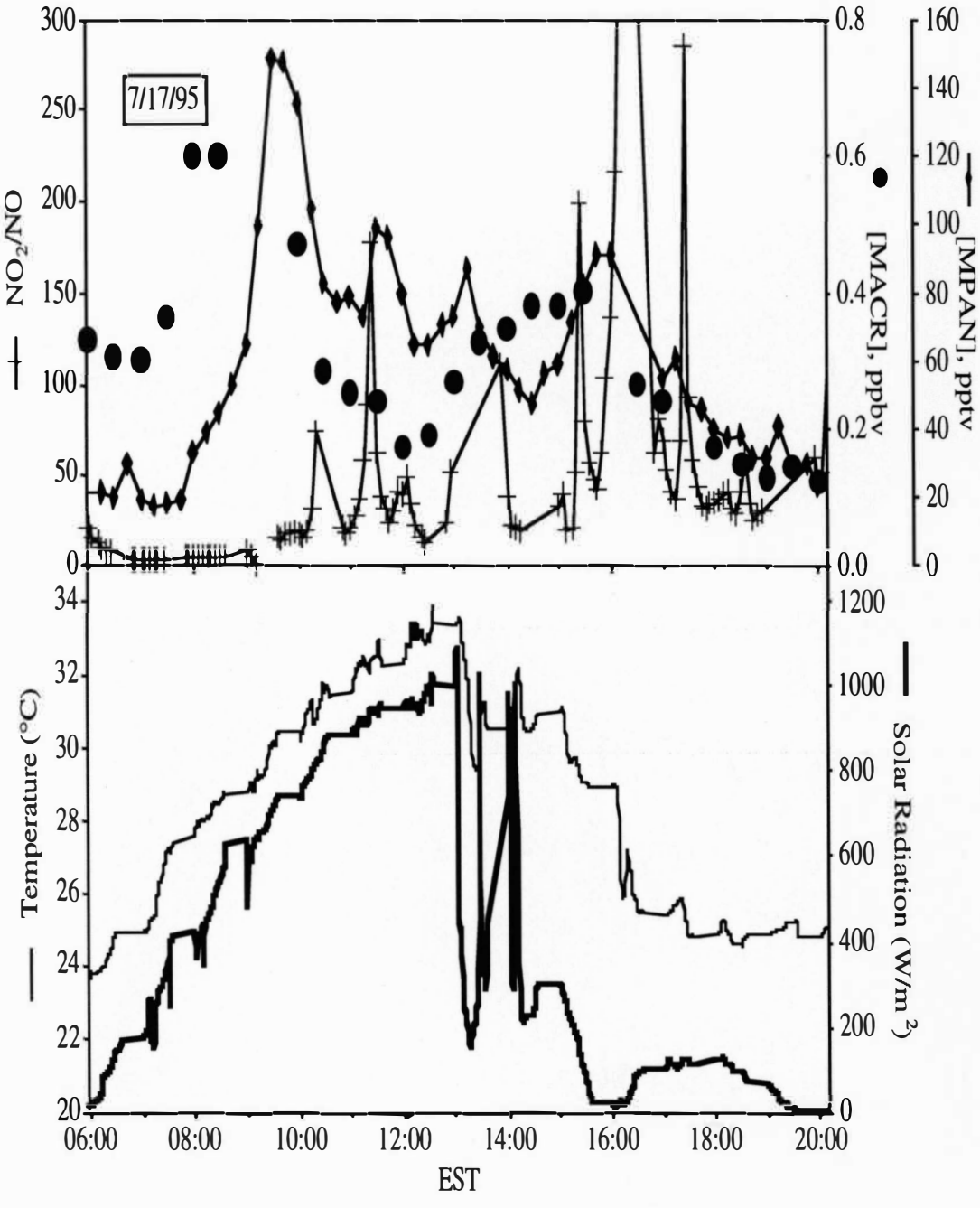

Figure 21. Timeseries Plots of MPAN, MACR, Preliminary NO_2/NO, Solar Flux and Temperature for July 17 When MPAN and MACR Were Poorly Correlated.

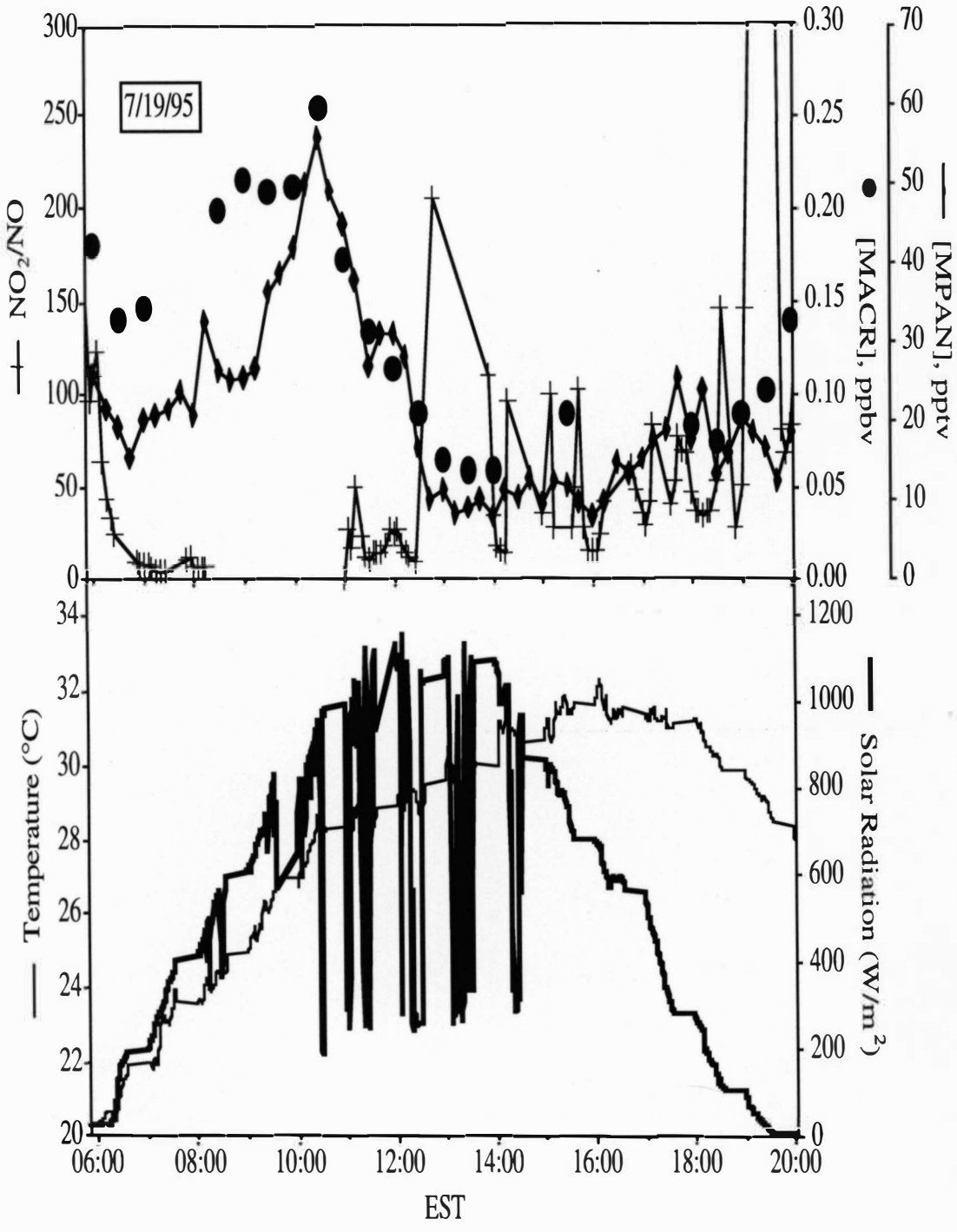

Figure 22. Timeseries Plots of MPAN, MACR, Preliminary NO_2/NO, Solar Flux and Temperature for July 19 When MPAN and MACR Correlated Well.

NOy increases during that time from 5 ppbv to 12 ppbv, which indicates that air is being transported from a more polluted region. At 1600 hours, a thunderstorm causes a power outage at the site which prevents collection of MPAN and MACR data and the temperature takes another drop to 25 ^{0}C. After 1630 hours, photochemical activity is minimal due to the very low solar flux and MPAN and MACR begin to decrease simultaneously. Hence, a combination of high NO_2/NO, high NO_2, low temperature, low solar flux and transport appear to influence the tracking between MPAN and MACR on July 17. The high NO_2 and low solar flux will lead to lower OH concentrations which slows down MACR production, while the high NO_2/NO and the low temperature will aid in increasing the lifetime of MPAN. On July 19, there are significantly lower MPAN, MACR and NO_2 concentrations, but the NO_2/NO ratios are similar on average. The day was relatively clear and warm with occasional clouds around mid-day. MPAN and MACR peak at the same time at 1030 hours. After peaking, MPAN and MACR track well through the afternoon. The apparent lower NO_2 concentrations on this sunnier day, compared to July 17, appear to be less effective in sinking OH radicals and therefore less likely to affect the tracking between MPAN and MACR whose production and destruction rates are dependent on OH radicals.

MPAN + OH Reaction

As suggested previously, the lifetime of MPAN may be influenced by the reactivity of its double bond toward O_3 and OH radicals. The lifetime of MPAN due to reaction with O_3 and OH is 14 hours and 7.7 hours respectively when [O_3] = 100 ppbv (Grosjean et al., 1993a) and [OH] = 10^7 molecules/cm^3 (Grosjean et al., 1993c). Although thermal decomposition will be the main loss process at typical summer temperatures and NO_2/NO ratios in Nashville, the effect of O_3 and OH on the lifetime

of MPAN may still be substantial. In this section, focus will be placed on the significance of the MPAN+OH reaction on the lifetime of MPAN under atmospheric conditions similar to those usually seen in the Nashville area during summer.

According to equations 12, 13 and 14, the change of MPAN concentrations with time is $d[MPAN]/dt = k_{-1}[MACROO][NO_2] - k_1[MPAN] - k_3[MPAN][OH]$.

$$MPAN \underset{k_{-1}}{\overset{k_1}{\rightleftharpoons}} MACROO + NO_2 \qquad (12)$$

$$MACROO + NO \xrightarrow{k_2} Products \qquad (13)$$

$$MPAN + OH \xrightarrow{k_3} Products \qquad (14)$$

A lifetime expression for MPAN can be derived from d[MPAN]/dt by assuming steady state in the peroxyacyl radical MACROO. This assumption is reasonable at Youth Inc. where reactions between peroxy radicals reactions may be minimal due to high NO_x levels. The derived lifetime expression (equation 15) may be used to examine the added effect of the OH reaction on MPAN thermal lifetime, where $k_{-1}/k_2 = 0.48$ (Atkinson et al, 1992), $k_3 = 3.6*10^{-12}$ cm^3/(molecules*sec) (Grosjean et al., 1993c) and $k_1 = 10^{16.2}e^{((-26.8\ Kcal/mol)/RT)}$ sec^{-1} (Roberts and Bertman, 1992). Figure 23 is a plot of

$$\tau = \frac{1}{k_3[OH] + \left(\frac{k_1}{\left(\frac{k_{-1}[NO_2]}{k_2[NO]} \right) + 1} \right)} \qquad (15)$$

the percent reduction in MPAN lifetime, as a function of NO_2/NO ratio, brought by the added reaction of MPAN with OH compared to thermal lifetime alone. This plot shows that although thermal decomposition is the main loss process for MPAN, the effect of

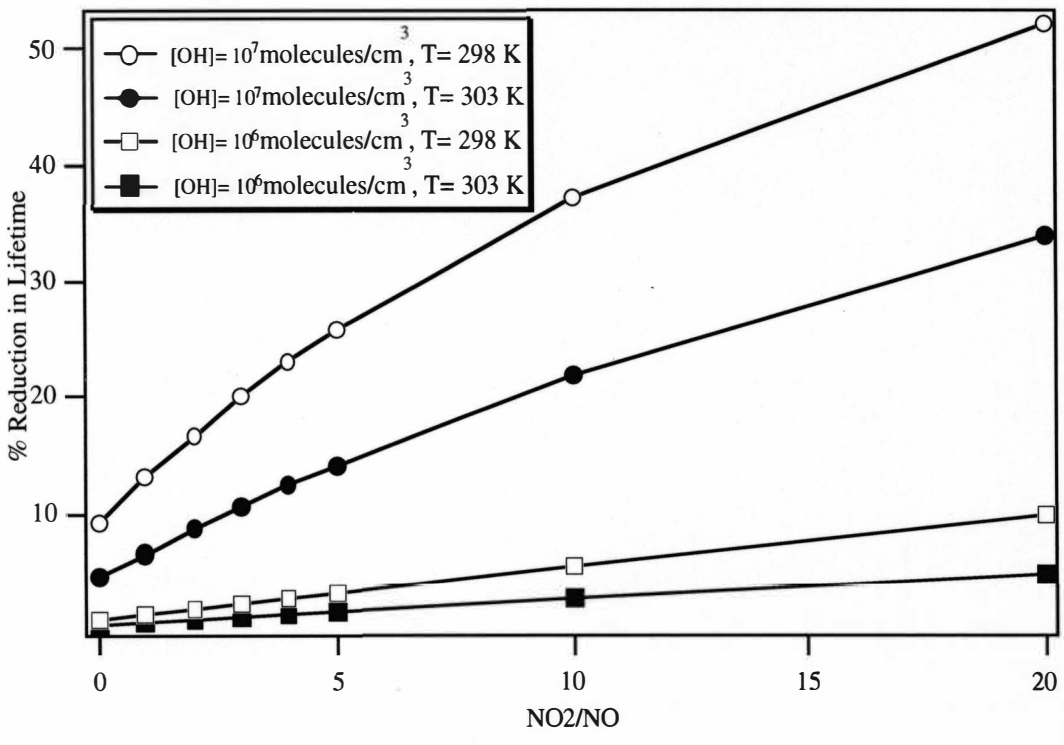

Figure 23. Percent Reduction in MPAN Lifetime in Addition to Thermal Decomposition Through the Reaction of MPAN With OH at 298K and 303K and OH Concentrations of 10^6 and 10^7 Molecules/cm^3.

OH on MPAN may be substantial at high OH concentrations, high NO_2/NO ratios and low temperatures provided that NO_2 concentration is not high enough to sink OH radicals and that the MPAN + OH reaction is not significantly temperature dependent. To put Figure 23 in context of conditions at Youth Inc in July, where average noon time temperatures were around 303 K, the daytime NO_2/NO median was approximately 10 and assuming an OH concentration of 10^7 molecules/cm^3, the OH reaction with MPAN could help reduce the lifetime of MPAN by about 22% to 1.7 hours compared to the thermal lifetime of 2.2 hours. At 298 K, the percent reduction in MPAN lifetime would increase to 37 %. Under conditions of high photoactivity like July 19, the OH reaction with MPAN may then be significant, although thermal decomposition would

still be the dominant loss process for MPAN. In the case of July 17, the removal of OH by high concentrations of NO_2 along with the high NO_2/NO ratio will increase the lifetime of MPAN.

CHAPTER V

CONCLUSIONS

A synthetic and purification procedure that provides MPAN calibration standards of adequate concentration and purity was described. This allowed the first simultaneous measurements of MPAN, MACR and isoprene. The PANs data at Youth Inc. was rich and complex, and displayed signs of active biogenic and anthropogenic photoproduction and transport. PAN is more often formed from anthropogenic than biogenic precursors as seen in the PPN vs. PAN and MPAN vs. PAN plots. All three PANs showed strong diurnal trends typical of flatlands where strong nocturnal inversion layers occur. The morning peaks in MACR and PANs are in part due to downward mixing as the NBL breaks up. MPAN has a shorter ambient lifetime than PAN and PPN as seen in the PANs diurnal plots and is more susceptible to attack by OH and O_3 due to its double bond. Unlike PAN, MPAN constituted a minute fraction of NOy and correlated least with O_3. The PAN/O_3 slope was smaller than what would be expected at remote sites despite the proximity of Youth Inc. to urban areas and this could be due to more efficient ozone formation from isoprene. On average during the day, MPAN and PPN tracked their precursors MACR and propanal with a slight delay, showing active photooxidation and dependence of PANs on their precursors. The periods when MPAN and MACR do not correlate are partly due to high NO_2, high NO_2/NO and lower OH production which decrease the production of MACR and increase the lifetime of MPAN. The shorter lifetime, lower concentrations, and lower NOy fractions imply that MPAN may not be a significant reservoir and transporter of NOx at Youth Inc. and that MPAN's production potential of ozone may be limited to a

local scale. This would make MPAN an effective indicator of local biogenic photochemistry considering that it has one mainly biogenic precursor, MACR.

Appendix A

Calculation of OH Formation Rate at λ= 308 Nanometers

The rate of formation of OH radicals was approximately calculated at 308 nm using total solar flux , ambient temperature, relative humidity, ambient pressure and ozone data from Youth Inc.. The rate of OH formation, $d[OH]/dt = 2\ J[O_3]/(1 + (k_2[M]/k_1[H_2O]))$, was derived from the following reactions by assuming steady state in O:

$$O_3 \xrightarrow{J} O(^1D) + O_2 \qquad (16)$$

$$O(^1D) + H_2O \xrightarrow{k_1} 2\ OH \qquad (17)$$

$$O(^1D) + M \xrightarrow{k_2} O(^3P) \qquad (18)$$

where k_1= 2.2e-10 $cm^3/(molecules*sec)$ (Atkinson et al., 1992) and k_2= $1.8*10^{-11}e(107/T)$ $cm^3/(molecules*sec)$ (Atkinson et al., 1992). The rate constant of O_3 photolysis, J, is equal to $\Sigma\ I(\lambda)*\sigma(\lambda)*\Phi(\lambda)$, where $I(\lambda)$ is the solar flux at wavelength λ in $(photons/cm^2)/sec$, $\sigma(\lambda)$ is the absorption cross section at wavelength λ in $cm^2/molecule$, and $\Phi(\lambda)$ is the quantum yield at wavelength λ. In order to determine d[OH]/dt at 308 nm using the above equation, J, [M], $[H_2O]$ needed to be calculated and the ambient ozone concentrations in ppbv had to be converted to $molecules/cm^3$.

Since the solar flux data collected at Youth Inc. were measured in $Watt/m^2$ at all wavelengths, it was necessary to convert the data to $(photons/cm^2)/sec$ at 308 nm. That was done as follows:

1. The zenith angles at different times of the day were gathered (Table 3.7, Finlayson-Pitts and Pitts, 1986) for July 1 for a latitude of 40 ^{0}N which was the closest latitude with data to the latitude of the Nashville area. Since the use of the resulting OH formation rate data was going to be qualitative in nature, a small difference in latitude was deemed insignificant.

2. Solar flux values in the 305-310 nm range were acquired (Table 3.5, Finlayson-Pitts and Pitts, 1986). These two tables allowed the interpolation for solar fluxes at 305-310 nm (photon/cm^2)/sec at different times of the day based on zenith angles. Figure 24 shows the observed mean diurnal solar flux at Youth Inc. (all wavelength) in Watts/m^2 and the calculated theoretical solar flux (305-310 nm) in (photons/cm^2)/sec in relatively good agreement. The slight difference in cycle duration may be due to one or combination of: a) differences between solar time (used in the calculated solar flux) and eastern standard time, EST, (used for the mean all-wavelength solar flux), b) differences due to latitude errors.

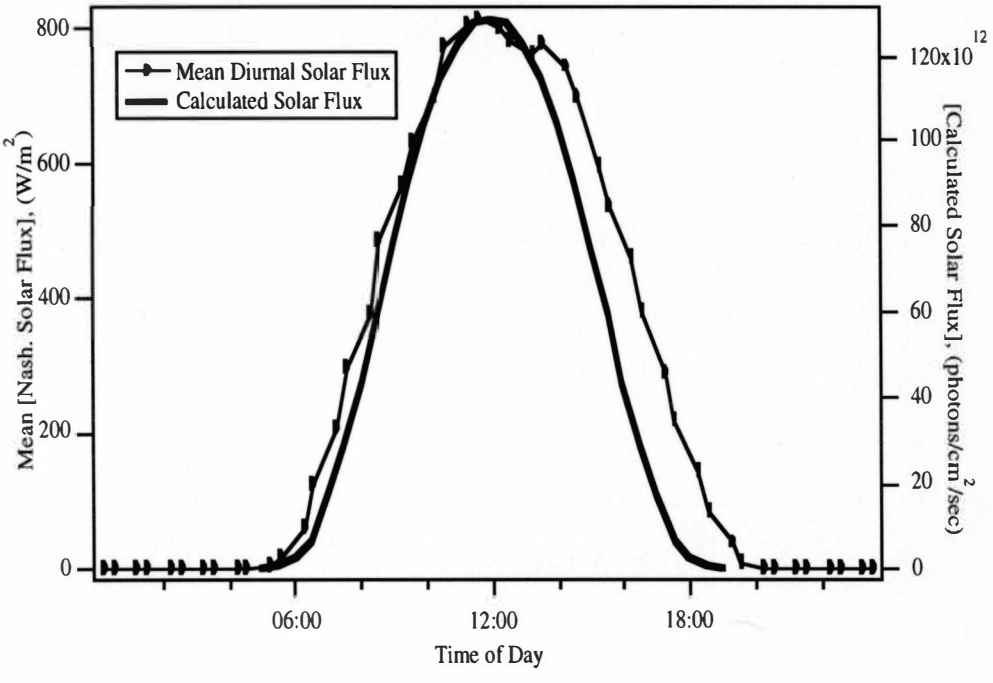

Figure 24. Plot of Mean Diurnal Solar Flux at Youth Inc. and the Calculated Theoretical Solar Flux Diurnal (305-310 nm) for July 1, 40°N Latitude.

3. A linear fit of the calculated theoretical solar flux values at 305-310 nm for July 1 at a latitude of 40 °N versus the mean diurnal solar flux data measured at Youth Inc. in Watts/m^2 for all wavelengths (Figure 25) gave a good correlation (R=0.979 for

n= 14 points) and the following equation: (Theoretical S.F. at 305-310 nm) = (1.6912e+11)*(Measured S.F.) - 1.8804e+13. This equation would allow the conversion of the all wavelength solar flux data at Youth Inc. from Watts/m^2 to (photons/cm^2)/sec at 305-310 nm.

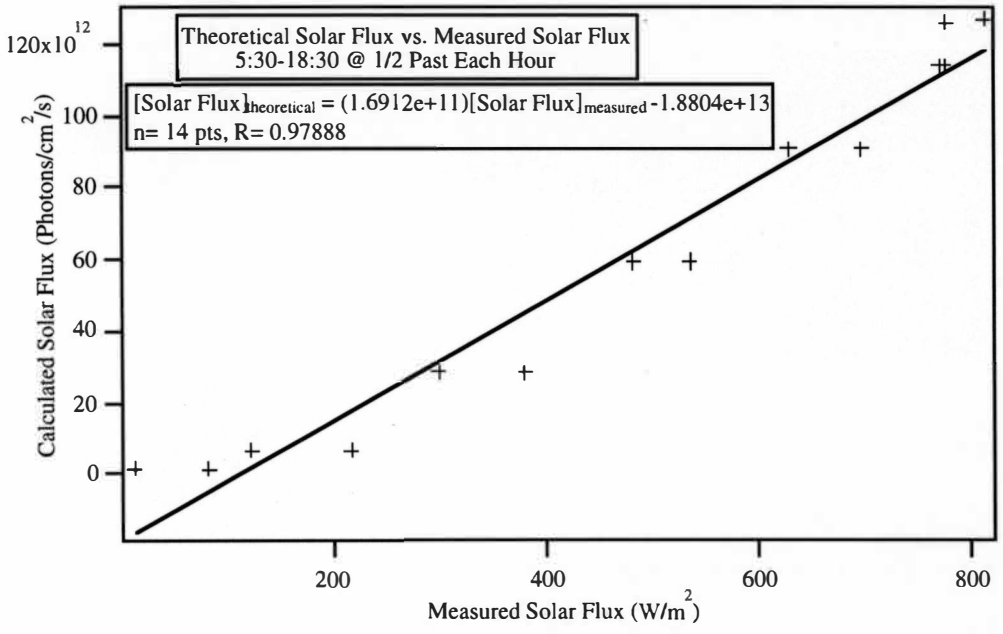

Figure 25. Theoretical Solar Flux (305-310 nm) for July 1, 40 °N Latitude Versus Measured Solar Flux at Youth, Inc..

4. The cross-section σ (308 nm) = 13.64*10^{-20} cm^2/molecule at 298 K (Molina and Molina, 1986) and the quantum yield Φ(308 nm)= 0.79 (Greenblatt and Wiesenfeld, 1983) were used along with the above conversion equation to calculate the photolysis rate constant of ozone at 308 nm, J = I(308 nm).σ (308 nm).Φ(308 nm), at different times of the day.

The concentration of air in moles/cm^3 at a particular ambient pressure and a particular measurement time was calculated using n= PV/RT, where V= 1 cc, P= ambient pressure in mbar, T= ambient temperature in degrees Kelvin, and R=

$83.14*10^3$ $(mbar*cm^3)/(K*mol)$. By multiplying the number of moles/cm^3 by $6.022*10^{23}$ mol^{-1} the concentration of air in molecules/ cm^3 was acquired. To calculate the ambient water number density, the vapor pressure of water was plotted versus temperature over the range of 15-40 °C (CRC, Handbook of Chemistry and Physics, 52nd Edition), which is approximately the temperature range observed at Youth Inc. during the entire measurement period (Figure 26). The data were then fitted to the following equation, Max. V.P. (mmHg) = $13.136 - 0.6229X + 0.041673X^2$, where X is the ambient temperature in degrees Celcius.

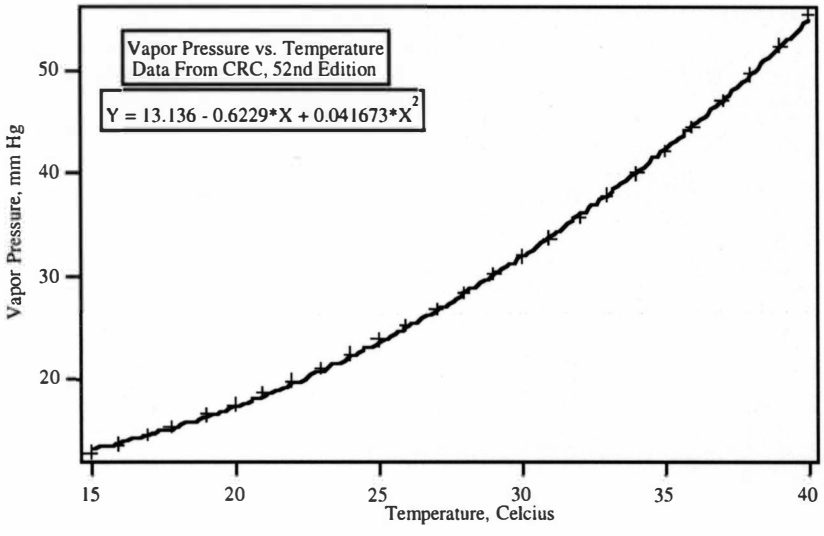

Figure 26. Maximum Water Vapor Pressure Versus Temperature in the 15-40 °C Range.

The ambient vapor pressure (V.P.) was then calculated using the equation: ambient V.P. = (R.H/100) * maximum vapor pressure, where R.H. is the relative humidity. Multiplying the concentration of air in molecules/cm^3 by (ambient V.P./Total ambient pressure) yielded the concentration of water vapor in molecules/cc. The concentration of ozone was converted from ppbv to molecules/cm^3 by multiplying the concentration in ppbv by 10^{-9} and by the concentration of air in molecules/cm^3 at ambient pressure.

BIBLIOGRAPHY

Altshuller, A.P., Measurements of the products of atmospheric photochemical reactions in laboratory studies and in ambient air - Relationships between ozone and other product, Atmos. Environ., 17, 2383-2427, (1983).

Altshuller, A.P., PANs in the Atmosphere, Air & Waste, 43, 1221, (1993).

Appel, B.R., A new and more sensitive procedure for analysis of peroxybenzoyl nitrate, J. Air Pollut. Contr. Ass., 23, 1042-1044, (1973).

Aschmann, S.M., and R. Atkinson, Formation yields of methyl vinyl ketone and methacrolein from the gas-phase reaction of O_3 with Isoprene, Environ. Sci. Technol., 28(8), 1539-1542, (1994).

Aschmann, S.M., Y. Shu, J. Arey, and R. Atkinson, Products of the gas-phase reactions of cis-3-hexen-1-ol with OH radicals and O_3, Atmos. Environ., 31, 3551-3560, (1997).

Atkinson, R, D.L. Baulch, R.A. Cox, R.F. Hampson, J.A. Kerr, and J. Troe, Evaluated kinetic and photochemical data for atmospheric chemistry. Supplement IV, J. Phys. Chem. Ref. Data, 21, 1125-1568, (1992).

Bertman, S.B., and J.M. Roberts, A PAN analog from isoprene photooxidation, Geophys. Res. Lett., 18(8), 1461-1464, (1991).

Biesenthal, T.A., and P.B. Shepson, Observations of anthropogenic inputs of the isoprene oxidation products methyl vinyl ketone and methacrolein to the atmosphere, Geophys. Res. Lett., 24, 1375-1378, (1997a).

Biesenthal, T.A., Q. Wu, P.B. Shepson, H.A. Wiebe, K.G. Anlauf, and G.I. Mackay, A study of relationships between isoprene, its oxidation products, and ozone, in the lower Fraser Valley, BC, Atmos. Environ., 31, 2049-2058, (1997b).

Chameides, W.L., and E.B. Cowling, The State of the Southern Oxidants Study (SOS): Policy-Relevant Findings in Ozone Pollution Research 1988-1994, Southern Oxidants Study (1995).

CRC, Handbook of Chemistry and Physics, 52nd Edition, p.D148.

Fahey, D.W., G. Hübler, D.D. Parrish, E.J. Williams, R.B. Norton, B.A. Ridley, H.B. Singh, S.C. Liu, and F.C. Fehsenfeld, "Reactive nitrogen species in the troposphere: Measurements of NO, NO_2, HNO_3, particulate nitrate, peroxyacetyl nitrate (PAN), O_3 and total reactive odd nitrogen (NO) at Niwot Ridge, Colorado, J. Geophys. Res., 91D, 9781-9793, (1986).

Fehsenfeld, F., J. Calvert, R. Fall, P. Goldan, A.B. Guenther, C.N. Hewitt, B. Lamb, S. Liu, M. Trainer, H. Westberg, and P. Zimmerman, Emissions of volatile organic compounds from vegetation and the implications for atmospheric chemistry, Global Biogeochemical Cycles, 6(4), 389-430, (1992).

Finlayson-Pitts, B.J., and J.N. Pitts Jr., Atmospheric Chemistry: Fundamentals and Experimental Techniques, John Wiley, New York, (1986).

Fung, K, and D. Grosjean, Peroxybenzoyl nitrate: measurement in smog chambers and urban air, Sci. Total Environ.,46, 29-40, (1985).

Gaffney, J.S., R. Fajer, G.I. Senum, and J.H. Lee, An improved procedure for high purity gaseous peroxyacyl nitrate production: use of heavy lipid solvents, Atmos. Environ., 18, 215-218, (1984).

Gaffney, J.S., N.A. Marley, and E.W. Prestbo, Peroxyacyl nitrates (PANs): their physical and chemical properties", The Handbook of Environmental Chemistry, 4(B), 1-38, (1989).

Garland, J.A., and S.A. Penkett, Absorption of peroxyacetyl nitrate and ozone by natural surfaces, Atmos. Environ., 10, 1127, (1976).

Greenblatt, G.D., and J.R. Wiesenfeld, Time-resolved resonance fluorescence studies of $O(^1D_2)$ yields in the photodissociation of O_3 at 248 and 308 nm, J. Chem. Phys., 78(8), 4924-4928, (1983).

Grosjean, D., Discussions- Worldwide ambient measurements of peroxyacetyl nitrate (PAN) and implications for plant injury", Atmos. Environ., 18, 1489-1492, (1984).

Grosjean, D., E. Grosjean, and E.L. Williams II, The reaction of ozone with MPAN, $CH_2=C(CH_3)C(O)OONO_2$, Env. Sci. Technol., 27, 2548-2552, (1993a).

Grosjean, D., E.L. Williams II, and E. Grosjean, A biogenic precursor of peroxypropionyl nitrate: Atmospheric oxidation of cis-3-Hexen-1-ol, Env. Sci. Technol., 27, 979-981, (1993b).

Grosjean, D., E.L. Williams II, and E. Grosjean, Gas phase reaction of the hydroxyl radical with the unsaturated peroxyacyl nitrate $CH_2=C(CH_3)C(O)OONO_2$, Int. J. Chem. Kinet., 25, 921-929, (1993c).

Heddle, J.A., P.B. Shepson, J.D. Gingerich, and K.W. So, Mutagenicity of peroxyacetyl nitrate (PAN) in vivo- tests for somatic mutations and chromosomal aberrations, Environ. Mol. Mutagen., 21, 58-66, (1993).

Kleindienst, T.E., P.B. Shepson, D.F. Smith, E.E. Hudgens, C.M. Nero, L.T. Cuppit, J.J. Bufalini, and L.D. Claxton, Comparison of mutagenic activities of several peroxyacyl nitrates, Environ. Mol. Mutagen., 16, 70, (1990).

Martin, R.S., H. Westberg, E. Allwine, L. Ashman, J.C. Farmer, B. Lamb, Measurement of isoprene and its atmospheric oxidation products in a central Pennsylvania deciduous forest, Journal of Atmospheric Chemistry, 13, 1-32, (1991).

Meijer, G.M. and H. Nieboer, Determination of peroxybenzoyl nitrate (PBzN) in ambient air, VDI-Berichte, 270, 55-56, (1976).

Molina, L.T. and M.J. Molina, Absolute absorption cross sections of ozone in the 185- to 350-nm wavelength range", J. Geophys. Res., 91, 14501-14508, (1986).

Montzka, S.A., M Trainer, P.D. Goldan, W.C. Kuster, and F.C. Fehsenfeld, Isoprene and its oxidation products, methyl vinyl ketone and methacrolein, in the rural troposphere, J. Geophys. Res., 98(D1), 1101-1111, (1993).

Nieboer, H., and J. van Ham, Peroxyacetyl nitrate (PAN) in relation to ozone and some meteorological parameters at Delft in the Netherlands, Atmos. Environ., 10, 115-120, (1976).

Nielsen, T., A.M. Hansen, and E.L. Thomsen, A convenient method for preparation of pure standards of peroxyacetyl nitrate for atmospheric analyses, Atmos. Environ., 16, 2447-2450, (1982).

The 1993 Tropospheric OH Photochemistry Experiment, J. Geophys. Res., 102, D5, 6169-6510, (1997).

Parrish, D.D., M.P. Buhr, M. Trainer, R.B. Norton, J.P. Shimshock, F.C. Fehsenfeld, K.G. Anlauf, J.W. Bottenheim, Y.Z. Tang, H.A. Wiebe, J.R. Roberts, R.L. Tanner, L. Newman, V.C. Bowersox, K.J. Olszyna, E.M. Bailey, M.O. Rodgers, T. Wang, H. Berresheim, U.K. Roychowdhury, and K.L. Demerjian, The total reactive oxidized nitrogen levels and the partitioning between the individual species at six rural sites in eastern North America, J. Geophys. Res., 98(2D), 2927-2939, (1993).

Ridley, B.A., J.D. Shetter, J.G. Walega, S. Madronich, C.M. Elsworth, F.E. Grahek, F.C. Fehsenfeld, R.B. Norton, D.D. Parrish, G. Hübler, M. Buhr, E.J. Williams, E.J. Allwine, and H.H. Westberg, The behavior of some organic nitrates at Boulder and Niwot Ridge, Colorado, J. Geophys. Res., 95D, 13949-13961, (1990).

Roberts, J.M., The atmospheric chemistry of organic nitrates, Atmos. Environ., 24A, 243, (1990).

Roberts, J.M., and S.B. Bertman, The thermal decomposition of peroxyacetic nitric anhydride (PAN) and peroxymethacrylic nitric anhydride (MPAN), Intl. J. Chem. Kinet., 24, 297-307, (1992).

Roberts, J.M., R.L. Tanner, L. Newman, V.C. Bowersox, J.W. Bottenheim, K.G. Anlauf, K.A. Brice, D.D. Parrish, F.C. Fehsenfeld, M.P. Buhr, J.F. Meagher,

and E.M. Bailey, Relationships between PAN and ozone at sites in eastern North America, J. Geophys. Res., 100D, 22821-22830, (1995).

Roberts, J.M., J. Williams, K. Baumann, M.P. Buhr, P.D. Goldan, J. Holloway, G. Hübler, W.C. Kuster, D.D. Parrish, T.B. Ryerson, M Trainer, E. Williams, F.C. Fehsenfeld, S.B. Bertman, G. Nouaime, C. Seaver, G. Grodzinsky, and M. Rodgers, Measurements of PAN, PPN and MPAN made during the 1994 and 1995 Nashville intensives of the Southern Oxidants Study: Implications for regional ozone production from biogenic hydrocarbons", Submitted J. Geophys. Res., (1997).

Schrimpf, W., K. Lienaerts, K.P. Müller, J. Rudolph, R. Neubert, W. Schüßler, and I. Levin, Dry deposition of peroxyacetyl nitrate (PAN): Determination of its deposition velocity at night from measurements of the atmospheric PAN and ^{222}radon concentration gradient, Geophys. Res. Lett., 23, 3599, (1996).

Scott, W.E., E.R. Stephens, P.L. Hanst, and R.C. Doerr, Further developments in the chemistry of the atmosphere, Proc. Am. Petrol. Inst. Sec.III, 37, 171, (1957).

Shepson, P.B., J.W. Bottenheim, D.R. Hastie, and A. Venkatram, Determination of the relative ozone and PAN deposition velocities at night, Geophys. Res. Lett., 8, 1121-1124, (1992a).

Shepson, P.B., D.R. Hastie, K.W. So, K.I. Schiff, Relationships between PAN, PPN and ozone at urban and rural sites in Ontario, Atmos. Environ., 26A, 1259-1270, (1992b).

Singh, H.B., and L.J. Salas, Measurements of peroxyacetyl nitrate (PAN) and peroxypropionyl nitrate (PPN) at selected urban, rural and remote sites, Atmos. Environ., 23, 231-238, (1989).

Sirois, A., and J.W. Bottenheim, Use of backward trajectories to interpret the 5-year record of PAN and O3 ambient air concentrations at Kejimkujik National Park, Nova Scotia, J. Geophys. Res., 100D, 2867-2881, (1995).

Starn, T.K., P.B. Shepson, S.B. Bertman, D.D. Riemer, R.G. Zika, K. Olszyna, Nighttime isoprene levels and chemistry at an urban-impacted forest site, Submitted, J. Geophys. Res., (1997a)

Starn, T.K., P.B. Shepson, S.B. Bertman, J.S. White, B.G. Splawn, D.D. Riemer, R.G. Zika, and K. Olszyna, Isoprene chemistry and its role in ozone production at a semi-rural site during the 1995 Southern Oxidants Study, Submitted, J. Geophys. Res., (1997b).

Stephens, E.R., The formation, reactions, and properties of peroxyacyl nitrates (PANs) in photochemical air pollution, Advances in Environmental Science and Technology, 1, 119, (1969).

Stephens, E.R., W.E. Scott, P.L. Hanst, and R.C. Doerr, R.C. Recent developments in the study of the organic chemistry of the atmosphere, JAPCA, 6, 159 (1956).

Temple, P.J., and P.C. Taylor, Worldwide ambient measurements of peroxyacetyl nitrate (PAN) and implications for plant injury, Atmos. Environ., 17, 1583-1587, (1983).

Tuazon, E.C., and R. Atkinson, A Product study of the gas-phase reaction of methacrolein with the OH radical in the presence of NO_x, Int. J. Chem. Kinet., 22, 591-602, (1990a).

Tuazon, E.C. and R. Atkinson, A product study of the gas-phase reaction of isoprene with the OH radical in the presence of NO_x, Int. J. Chem. Kinet., 22, 1221-1236, (1990b).

Williams, E.J., J.M. Roberts, K. Baumann, S.B. Bertman, S. Buhr, R.B. Norton, and F.C. Fehsenfeld, Variations in NOy composition at Idaho Hill, Colorado, J. Geophys. Res., 102D, 6297-6314, (1997a).

Williams, E.L., E. Grosjean, and D. Grosjean, Ambient levels of the peroxyacyl nitrates PAN, PPN and MPAN in Atlanta GA, J. Air Waste Manage Assoc., 43, 873, (1993).

Williams, J., J.M. Roberts, F.C. Fehsenfeld, S.B. Bertman, M.P. Buhr, P.D. Goldan, G. Hübler, W.C. Kuster, T.B. Ryerson, M. Trainer, and V. Young,Regional ozone from biogenic hydrocarbons deduced from airborne measurements of PAN, PPN, and MPAN, Geophys. Res. Lett., 24(9), 1099-1102, (1997b).